Light-Meson Spectroscopy with COMPASS

Boris Grube

Institute for Hadronic Structure and Fundamental Symmetries
Technische Universität München
Garching, Germany

Workshop on Bound States in Strongly Coupled Systems
Galileo Galilei Institute for Theoretical Physics
Florence, 15.03.2018

Light-Meson Spectrum

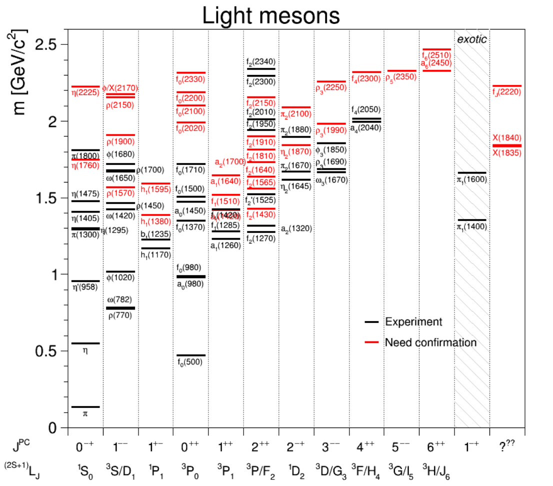

[Courtesy K. Götzen, GSI]

"Light-meson frontier"

- Many states need confirmation in mass region $m \gtrsim 2\,\mathrm{GeV}/c^2$
- Many wide states $\Rightarrow$ overlap and mixing
- Identification of higher excitations becomes exceedingly difficult

Main focus of current COMPASS program

Light-Meson Spectrum

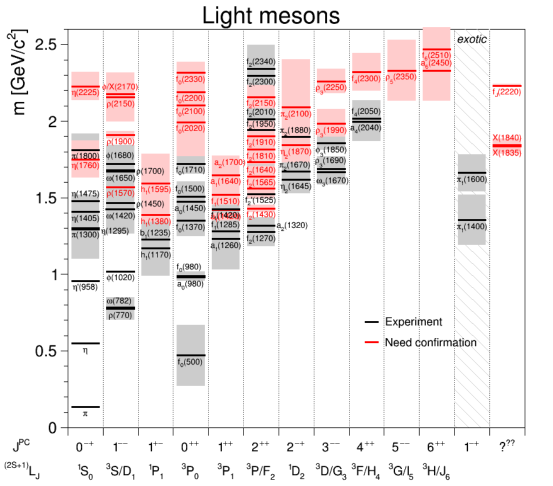

[Courtesy K. Götzen, GSI]

"Light-meson frontier"

- Many states need confirmation in mass region $m \gtrsim 2\,\mathrm{GeV}/c^2$
- Many wide states $\Rightarrow$ overlap and mixing
- Identification of higher excitations becomes exceedingly difficult

Main focus of current COMPASS program

Light-Meson Spectrum

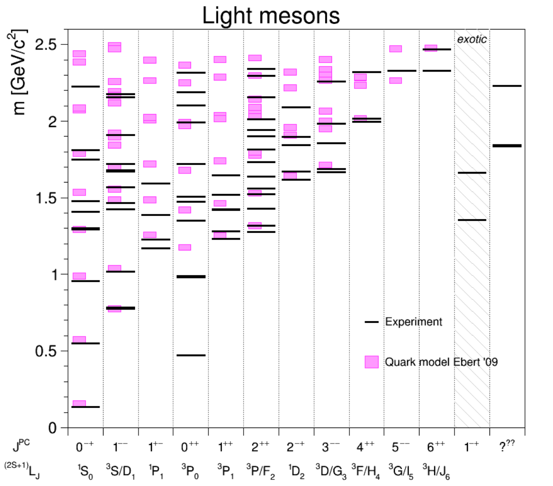

[Courtesy K. Götzen, GSI]

"Light-meson frontier"

- Many states need confirmation in mass region $m \gtrsim 2\,\text{GeV}/c^2$
- Many wide states $\Rightarrow$ overlap and mixing
- Identification of higher excitations becomes exceedingly difficult

Main focus of current COMPASS program

Light-Meson Spectrum

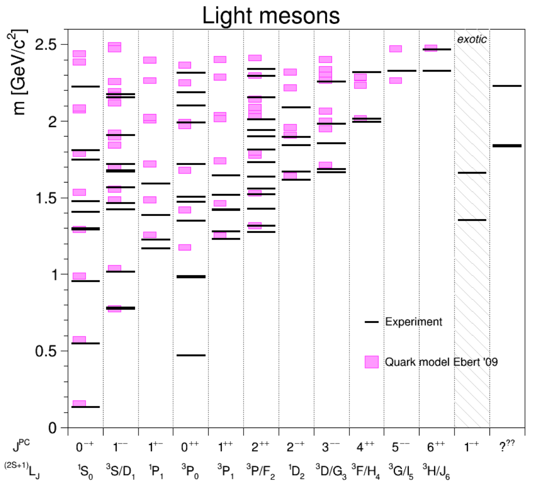

[Courtesy K. Götzen, GSI]

"Light-meson frontier"

- Many states need confirmation in mass region $m \gtrsim 2\,\mathrm{GeV}/c^2$
- Many wide states $\Rightarrow$ overlap and mixing
- Identification of higher excitations becomes exceedingly difficult

Main focus of current COMPASS program

Beyond the Constituent Quark Model

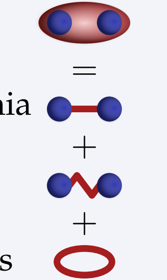

$=$

Quarkonia $|q\bar{q}\rangle$

$+$

Hybrids $|q\bar{q}g\rangle$

$+$

Glueballs $|gg\rangle$

$+$

Multi-quarks $|q^2\bar{q}^2\rangle$

$+$

$\vdots$

QCD permits additional color-neutral configurations

- *Physical mesons:* linear superpositions of *all* allowed basis states
- Amplitudes in principle determined by QCD interactions
- Disentanglement of contributions difficult
- *Light mesons:* no definitive experimental evidence yet

Beyond the Constituent Quark Model

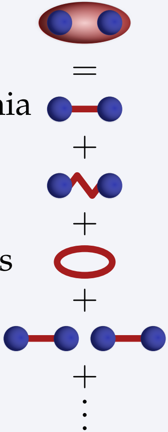

	=	
Quarkonia		$\lvert q\bar{q}\rangle$
	+	
Hybrids		$\lvert q\bar{q}g\rangle$
	+	
Glueballs		$\lvert gg\rangle$
	+	
Multi-quarks		$\lvert q^2\bar{q}^2\rangle$
	+	
	$\vdots$	

QCD permits additional color-neutral configurations

- *Physical mesons:* linear superpositions of *all* allowed basis states
- Amplitudes in principle determined by QCD interactions
- Disentanglement of contributions difficult
- *Light mesons:* no definitive experimental evidence yet

State-of-the-art calculation with $m_\pi = 391\ \mathrm{MeV}/c^2$

Dudek *et al.*, PRD **88** (2013) 094505

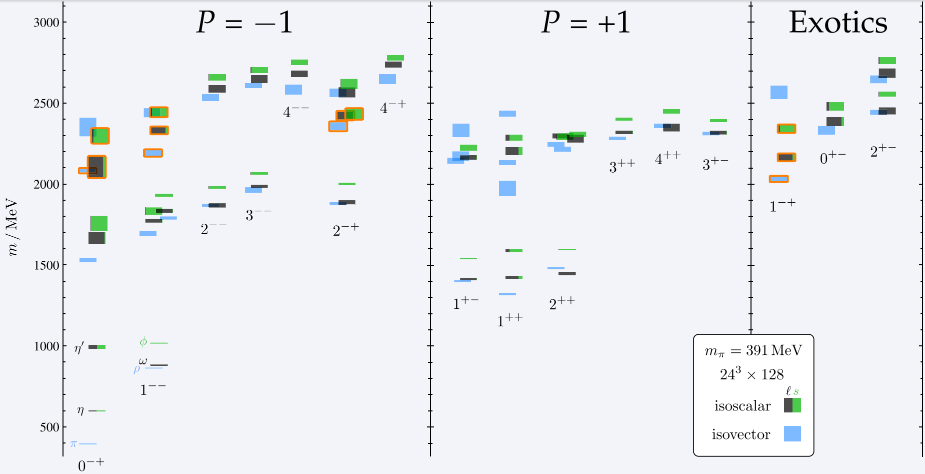

- High towers of excited states
- Essentially recovers quark-model pattern
- Additional hybrid-meson super-multiplet

C. Adolph *et al.*, NIMA **779** (2015) 69

Fixed-target experiment

- Two-stage spectrometer
- Large acceptance over wide kinematic range
- Electromagnetic and hadronic calorimeters
- Beam and final-state particle ID (CEDARs, RICH)

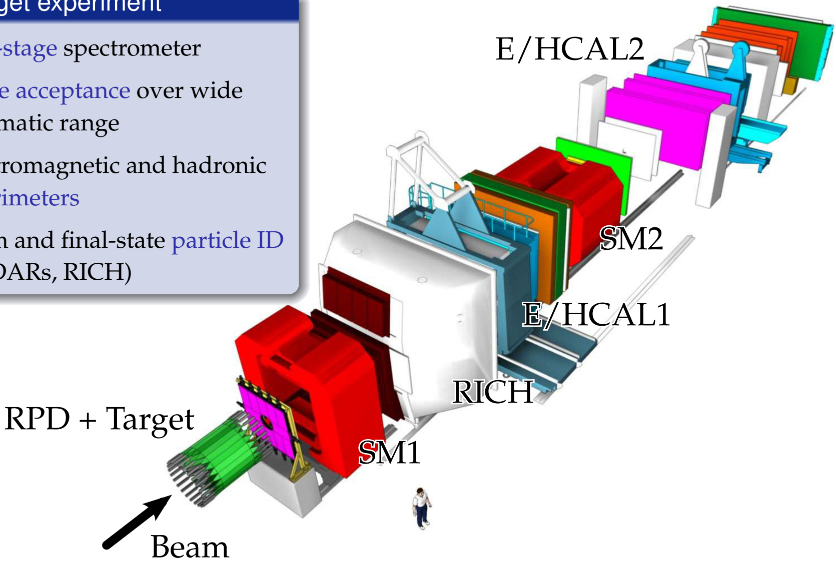

C. Adolph *et al.*, NIMA **779** (2015) 69

Fixed-target experiment

- Two-stage spectrometer
- Large acceptance over wide kinematic range
- Electromagnetic and hadronic calorimeters
- Beam and final-state particle ID (CEDARs, RICH)

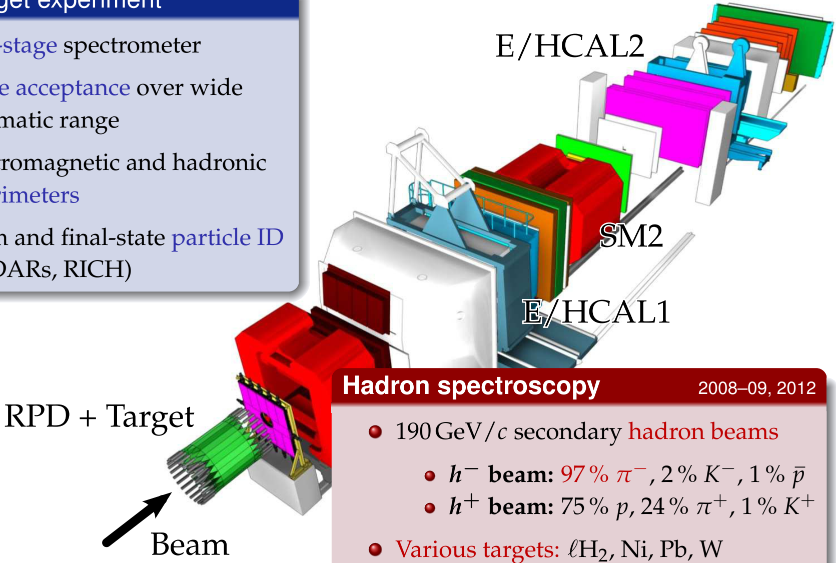

Hadron spectroscopy 2008–09, 2012

- 190 GeV/c secondary hadron beams
  - h^- **beam:** $97\,\%\ \pi^-$, $2\,\%\ K^-$, $1\,\%\ \bar{p}$
  - h^+ **beam:** $75\,\%\ p$, $24\,\%\ \pi^+$, $1\,\%\ K^+$
- Various targets: ℓH_2, Ni, Pb, W

C. Adolph *et al.*, NIMA **779** (2015) 69

Fixed-target experiment

- Two-stage spectrometer
- Large acceptance over wide kinematic range
- Electromagnetic and hadronic calorimeters
- Beam and final-state particle ID (CEDARs, RICH)

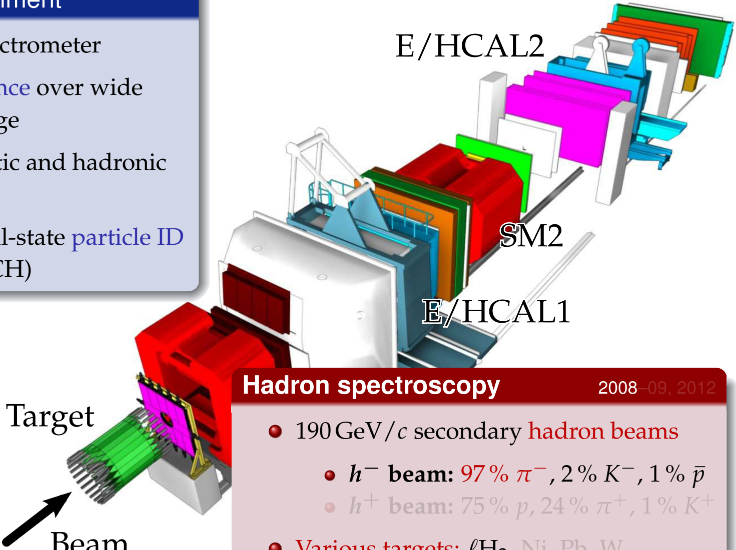

Hadron spectroscopy 2008–09, 2012

- $190\,\mathrm{GeV}/c$ secondary hadron beams
  - h^- **beam:** $97\,\%\ \pi^-, 2\,\%\ K^-, 1\,\%\ \bar{p}$
  - h^+ **beam:** $75\,\%\ p, 24\,\%\ \pi^+, 1\,\%\ K^+$
- Various targets: ℓH_2, Ni, Pb, W

Meson Production in Diffractive Dissociation

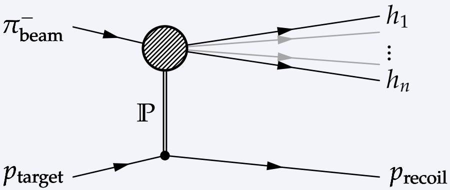

- Soft scattering of beam particle off target
  - Production of n forward-going hadrons
  - Target particle stays intact
- 190 GeV/c beam momentum $\Rightarrow$ interaction dominated by space-like Pomeron exchange
- All final-state particles are measured

Meson Production in Diffractive Dissociation

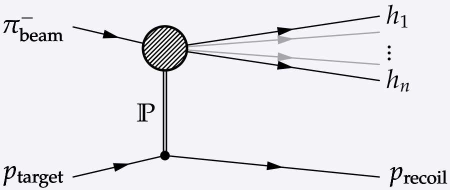

- Beam particle gets excited into intermediate resonances X
- X dissociate into n-body hadronic final state
- Rich spectrum of interfering intermediate states X

Goal: disentangle all contributing resonances X

- Determine their mass, width, and quantum numbers

Method: **partial-wave analysis** (PWA)

- Exploits full kinematic information of events
- *Amplitude analysis:* interference of intermediate states
  - Additional phase information increases sensitivity

Meson Production in Diffractive Dissociation

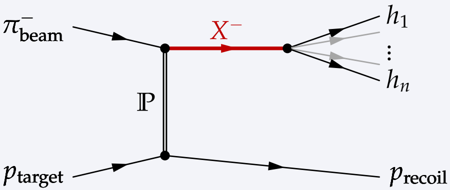

- Beam particle gets excited into intermediate resonances X
- X dissociate into n-body hadronic final state
- Rich spectrum of interfering intermediate states X

Goal: disentangle all contributing resonances X

- Determine their mass, width, and quantum numbers

Method: **partial-wave analysis** (PWA)

- Exploits full kinematic information of events
- *Amplitude analysis:* interference of intermediate states
  - Additional phase information increases sensitivity

Meson Production in Diffractive Dissociation

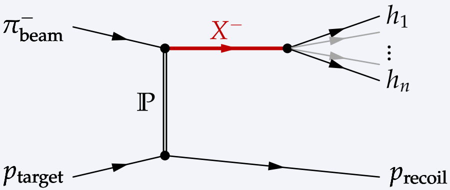

- Beam particle gets excited into intermediate resonances X
- X dissociate into n-body hadronic final state
- Rich spectrum of interfering intermediate states X

Goal: disentangle all contributing resonances X

- Determine their mass, width, and quantum numbers

Method: **partial-wave analysis** (PWA)

- Exploits full kinematic information of events
- *Amplitude analysis:* interference of intermediate states
  - Additional phase information increases sensitivity

Meson Production in Diffractive Dissociation

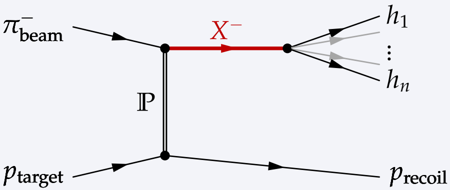

- Beam particle gets excited into intermediate resonances X
- X dissociate into n-body hadronic final state
- Rich spectrum of interfering intermediate states X

Goal: disentangle all contributing resonances X

- Determine their mass, width, and quantum numbers

Method: **partial-wave analysis** (PWA)

- Exploits full kinematic information of events
- *Amplitude analysis:* interference of intermediate states
  - Additional phase information increases sensitivity

Meson Production in Diffractive Dissociation

Example: $\pi^-\pi^-\pi^+$ final state

C. Adolph *et al.*, PRD **95** (2017) 032004

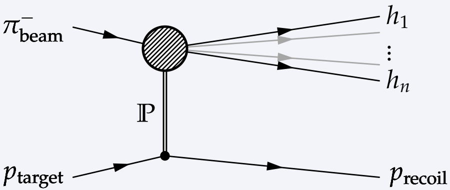

- Exclusive measurement
  - Clean data sample
- Squared four-momentum transfer $0.1 < t' < 1.0\,(\mathrm{GeV}/c)^2$
- 46×10^6 $\pi^-\pi^-\pi^+$ events
- Well-known 3π resonances appear in $m_{3\pi}$ spectrum

Meson Production in Diffractive Dissociation

Example: $\pi^-\pi^-\pi^+$ final state

C. Adolph *et al.*, PRD **95** (2017) 032004

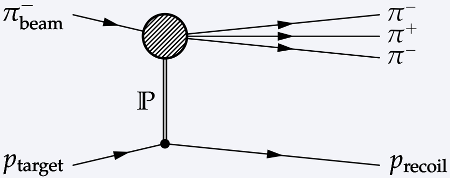

- Exclusive measurement
  - Clean data sample
- Squared four-momentum transfer $0.1 < t' < 1.0\,(\mathrm{GeV}/c)^2$
- 46×10^6 $\pi^-\pi^-\pi^+$ events
- Well-known 3π resonances appear in $m_{3\pi}$ spectrum

Meson Production in Diffractive Dissociation

Example: $\pi^-\pi^-\pi^+$ final state

C. Adolph *et al.*, PRD **95** (2017) 032004

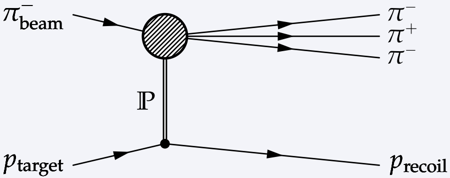

- Exclusive measurement
  - Clean data sample
- Squared four-momentum transfer $0.1 < t' < 1.0\,(\mathrm{GeV}/c)^2$
- 46×10^6 $\pi^-\pi^-\pi^+$ events
- Well-known 3π resonances appear in $m_{3\pi}$ spectrum

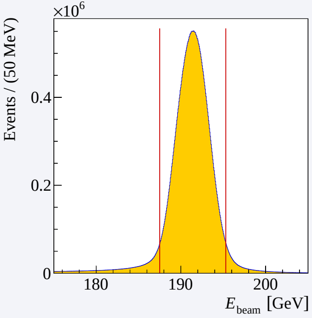

Meson Production in Diffractive Dissociation

Example: $\pi^-\pi^-\pi^+$ final state — C. Adolph *et al.*, PRD **95** (2017) 032004

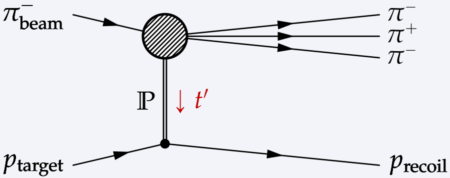

- Exclusive measurement
  - Clean data sample
- Squared four-momentum transfer
  $0.1 < t' < 1.0\ (\text{GeV}/c)^2$
- $46 \times 10^6\ \pi^-\pi^-\pi^+$ events
- Well-known 3π resonances appear in $m_{3\pi}$ spectrum

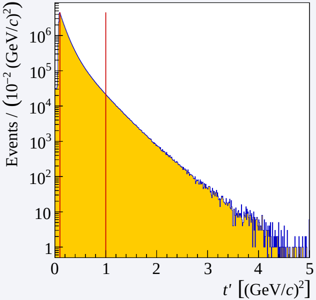

Meson Production in Diffractive Dissociation

Example: $\pi^-\pi^-\pi^+$ final state

C. Adolph *et al.*, PRD **95** (2017) 032004

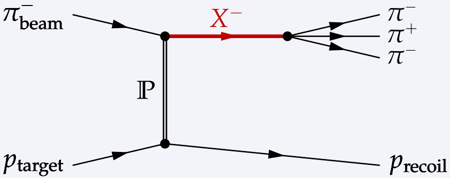

- Exclusive measurement
  - Clean data sample
- Squared four-momentum transfer $0.1 < t' < 1.0\,(\text{GeV}/c)^2$
- 46×10^6 $\pi^-\pi^-\pi^+$ events
- Well-known 3π resonances appear in $m_{3\pi}$ spectrum

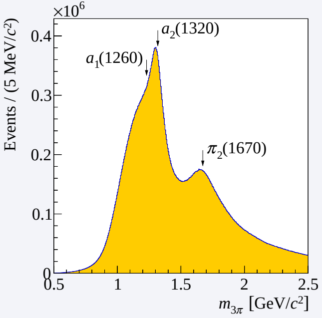

Meson Production in Diffractive Dissociation

Example: $\pi^-\pi^-\pi^+$ final state

C. Adolph *et al.*, PRD **95** (2017) 032004

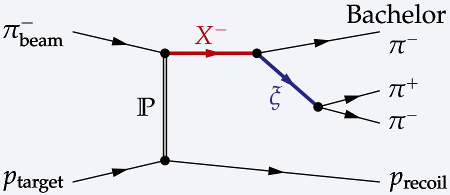

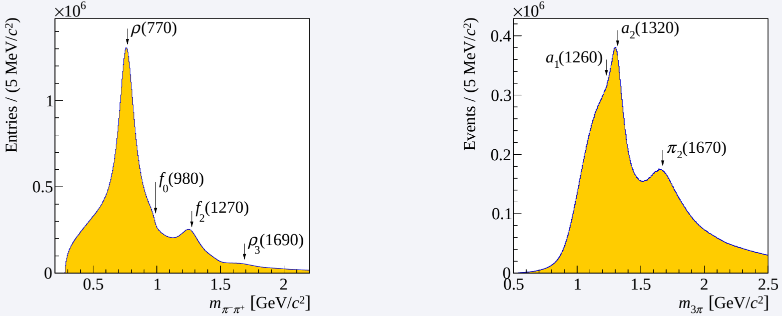

Decay of X via intermediate $\pi^-\pi^+$ resonances = "isobars"

Meson Production in Diffractive Dissociation

Example: $\pi^-\pi^-\pi^+$ final state

C. Adolph *et al.*, PRD **95** (2017) 032004

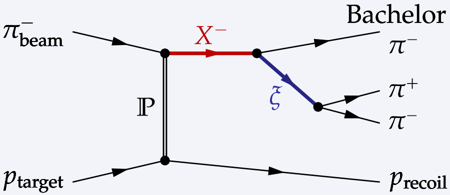

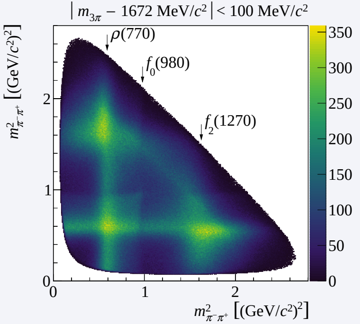

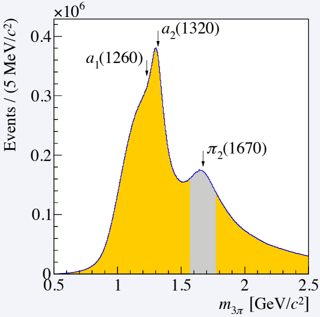

Decay of X via intermediate $\pi^-\pi^+$ resonances = "isobars"

Partial-Wave Decomposition of $\pi^-\pi^-\pi^+$ Final State

C. Adolph *et al.*, PRD **95** (2017) 032004

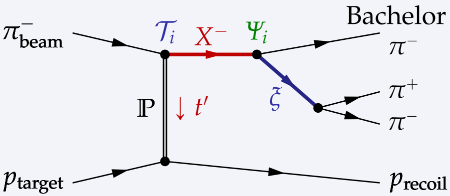

Ansatz: Factorization of production and decay

$$\mathrm{d}\sigma \propto \left| \sum_i^{\text{waves}} \mathcal{T}_i(m_{3\pi}, t')\, \Psi_i(m_{3\pi}, \tau) \right|^2 \mathrm{d}m_{3\pi}^2\ \mathrm{d}t'\ \mathrm{dLIPS}_3(m_{3\pi}, \tau)$$

- Fit model: coherent sum of partial-wave amplitudes
- Decay amplitudes $\Psi_i(m_{3\pi}, \tau)$
  - Describe 5-dimensional τ distribution of partial waves
  - Calculated using isobar model and helicity formalism
- Transition amplitudes $\mathcal{T}_i(m_{3\pi}, t')$ $\Rightarrow$ **interesting physics**
  - Dependence on $m_{3\pi}$ and t' unknown
  - Extracted from data: PWA fits in narrow $m_{3\pi}$ and t' bins

Partial-Wave Decomposition of $\pi^-\pi^-\pi^+$ Final State

C. Adolph *et al.*, PRD **95** (2017) 032004

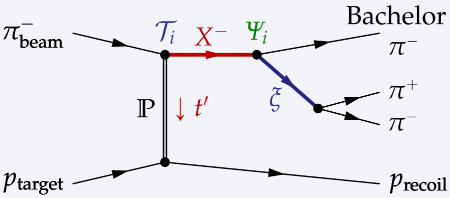

Ansatz: Factorization of production and decay

$$\mathrm{d}\sigma \propto \left| \sum_i^{\text{waves}} \mathcal{T}_i(m_{3\pi}, t')\, \Psi_i(m_{3\pi}, \tau) \right|^2 \mathrm{d}m^2_{3\pi}\ \mathrm{d}t'\ \mathrm{dLIPS}_3(m_{3\pi}, \tau)$$

- Fit model: coherent sum of partial-wave amplitudes
- Decay amplitudes $\Psi_i(m_{3\pi}, \tau)$
  - Describe 5-dimensional τ distribution of partial waves
  - Calculated using isobar model and helicity formalism
- Transition amplitudes $\mathcal{T}_i(m_{3\pi}, t')$ $\Rightarrow$ **interesting physics**
  - Dependence on $m_{3\pi}$ and t' unknown
  - Extracted from data: PWA fits in narrow $m_{3\pi}$ and t' bins

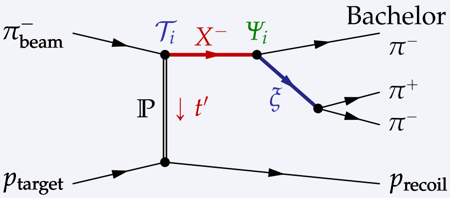

Ansatz: Factorization of production and decay

$$\mathrm{d}\sigma \propto \left| \sum_i^{\text{waves}} \mathcal{T}_i(m_{3\pi}, t')\, \Psi_i(m_{3\pi}, \tau) \right|^2 \mathrm{d}m_{3\pi}^2\; \mathrm{d}t'\; \mathrm{dLIPS}_3(m_{3\pi}, \tau)$$

- Fit model: coherent sum of partial-wave amplitudes
- Decay amplitudes $\Psi_i(m_{3\pi}, \tau)$
  - Describe 5-dimensional τ distribution of partial waves
  - Calculated using isobar model and helicity formalism
- Transition amplitudes $\mathcal{T}_i(m_{3\pi}, t') \Rightarrow$ interesting physics
  - Dependence on $m_{3\pi}$ and t' unknown
  - Extracted from data: PWA fits in narrow $m_{3\pi}$ and t' bins

Partial-Wave Decomposition of $\pi^-\pi^-\pi^+$ Final State

C. Adolph *et al.*, PRD **95** (2017) 032004

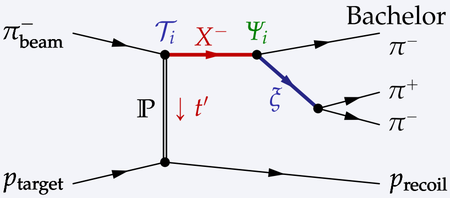

Ansatz: Factorization of production and decay

$$\mathrm{d}\sigma \propto \left| \sum_i^{\text{waves}} \mathcal{T}_i(m_{3\pi}, t')\, \Psi_i(m_{3\pi}, \tau) \right|^2 \mathrm{d}m_{3\pi}^2\ \mathrm{d}t'\ \mathrm{dLIPS}_3(m_{3\pi}, \tau)$$

- Fit model: coherent sum of partial-wave amplitudes
- Decay amplitudes $\Psi_i(m_{3\pi}, \tau)$
  - Describe 5-dimensional τ distribution of partial waves
  - Calculated using isobar model and helicity formalism
- Transition amplitudes $\mathcal{T}_i(m_{3\pi}, t')$ $\Rightarrow$ **interesting physics**
  - Dependence on $m_{3\pi}$ and t' unknown
  - Extracted from data: PWA fits in narrow $m_{3\pi}$ and t' bins

C. Adolph *et al.*, PRD **95** (2017) 032004

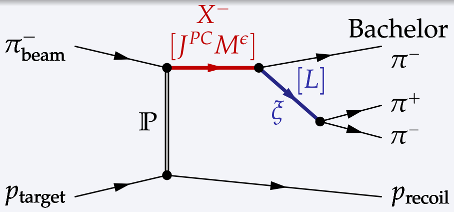

Fit model

- Included isobar resonances:
  - $[\pi\pi]_S$ $\quad J^{PC} = 0^{++}$
  - $\rho(770)$ $\quad 1^{--}$
  - $f_0(980)$ $\quad 0^{++}$
  - $f_2(1270)$ $\quad 2^{++}$
  - $f_0(1500)$ $\quad 0^{++}$
  - $\rho_3(1690)$ $\quad 3^{--}$
- Requires precise knowledge of isobar $\to \pi^-\pi^+$ amplitudes

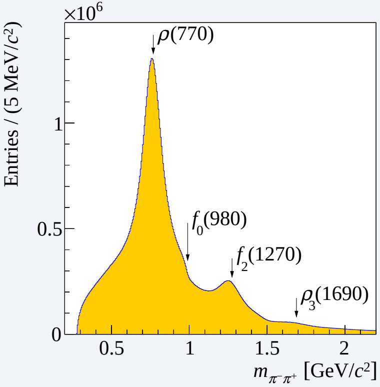

Partial-Wave Decomposition of $\pi^-\pi^-\pi^+$ Final State

C. Adolph *et al.*, PRD **95** (2017) 032004

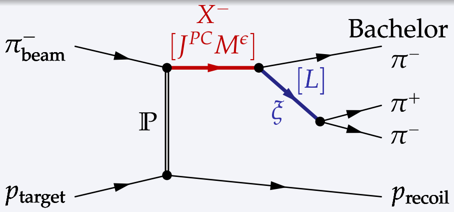

Fit model

- Included isobar resonances:
  - $[\pi\pi]_S$ $\quad J^{PC} = 0^{++}$
  - $\rho(770)$ $\quad 1^{--}$
  - $f_0(980)$ $\quad 0^{++}$
  - $f_2(1270)$ $\quad 2^{++}$
  - $f_0(1500)$ $\quad 0^{++}$
  - $\rho_3(1690)$ $\quad 3^{--}$
- Requires precise knowledge of isobar $\to \pi^-\pi^+$ amplitudes

- *Notation:* $J^{PC}\, M^\epsilon\, \xi\, \pi\, L$
- J and L up to 6
- 87 partial waves
- Additional incoherent isotropic background wave

Partial-Wave Decomposition of $\pi^-\pi^-\pi^+$ Final State

C. Adolph *et al.*, PRD **95** (2017) 032004

- Partial-wave decomposition performed independently in narrow $m_{3\pi}$ and t' bins
  - In each bin: fit to measured 5-dimensional intensity distribution
  - *Result:* transition amplitudes $\mathcal{T}_{\text{wave}}(m_{3\pi}, t')$
- PWA makes no assumptions about 3π resonances

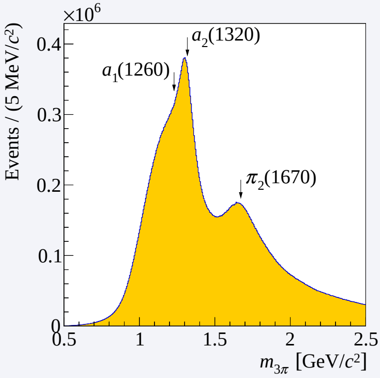

Partial-Wave Decomposition of $\pi^-\pi^-\pi^+$ Final State

C. Adolph *et al.*, PRD **95** (2017) 032004

- Partial-wave decomposition performed independently in narrow $m_{3\pi}$ and t' bins
  - In each bin: fit to measured 5-dimensional intensity distribution
  - *Result:* transition amplitudes $\mathcal{T}_{\text{wave}}(m_{3\pi}, t')$
- PWA makes no assumptions about 3π resonances

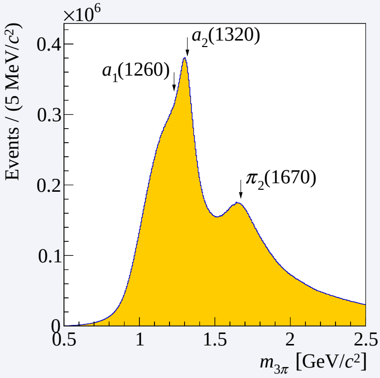

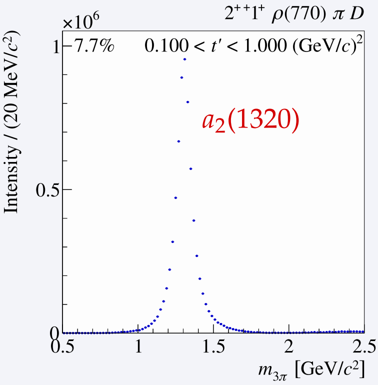

PWA $\pi^-\pi^-\pi^+$ Final State: Major Waves

C. Adolph *et al.*, PRD **95** (2017) 032004

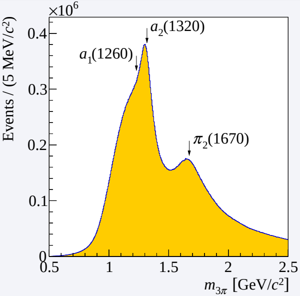

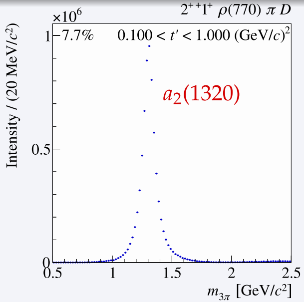

PWA $\pi^-\pi^-\pi^+$ Final State: Major Waves

C. Adolph *et al.*, PRD **95** (2017) 032004

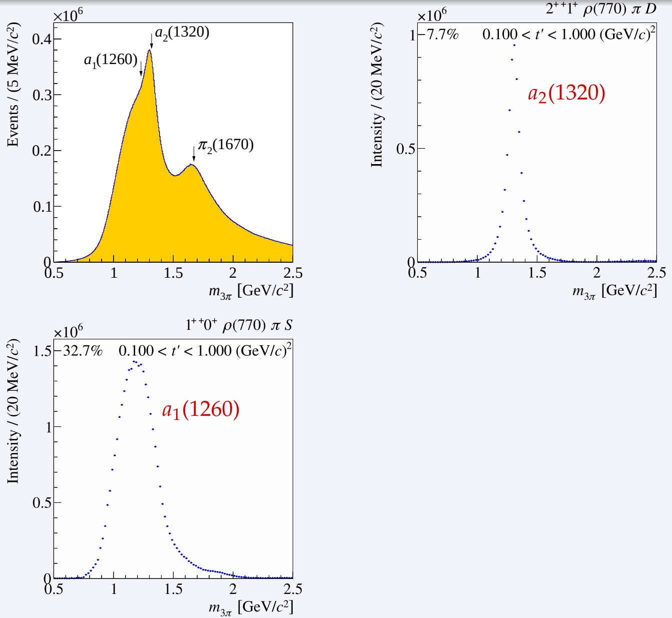

PWA $\pi^-\pi^-\pi^+$ Final State: Major Waves

C. Adolph *et al.*, PRD **95** (2017) 032004

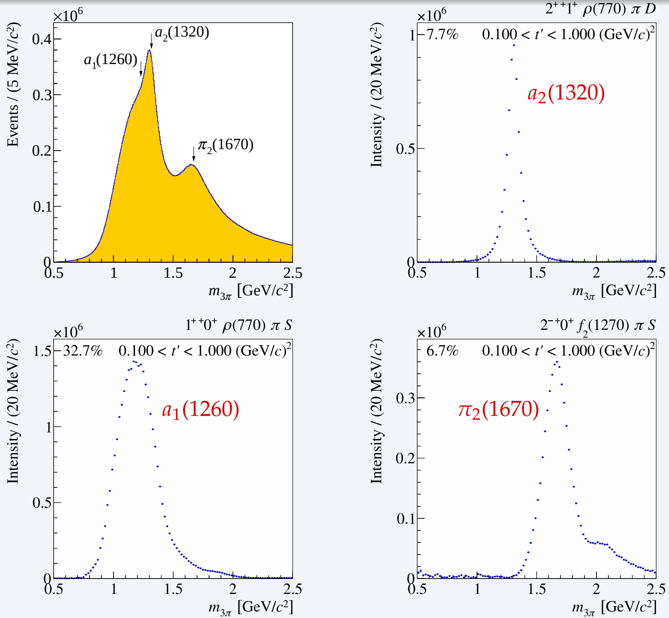

PWA $\pi^-\pi^-\pi^+$ Final State: Extraction of Resonances

[arXiv:1802.05913]

Experimental signatures of a resonance

- Intensity peak at resonance mass
- Phase motion: ϕ rises from 0° to 180° and is 90° at peak position
- Resonance mass and width are independent of four-momentum transfer t'

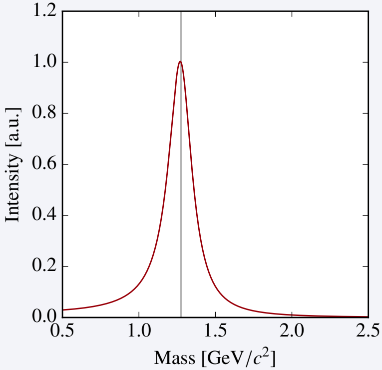

Experimental signatures of a resonance

- Intensity peak at resonance mass
- Phase motion: ϕ rises from 0° to 180° and is 90° at peak position
- Resonance mass and width are independent of four-momentum transfer t'

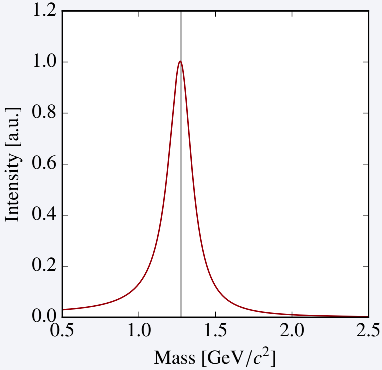

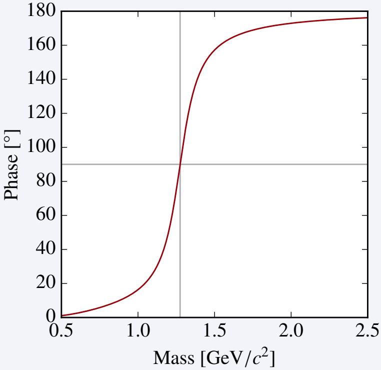

PWA $\pi^-\pi^-\pi^+$ Final State: Extraction of Resonances

[arXiv:1802.05913]

Experimental signatures of a resonance

- Intensity peak at resonance mass
- Phase motion: ϕ rises from 0° to 180° and is 90° at peak position
- Resonance mass and width are independent of four-momentum transfer t'

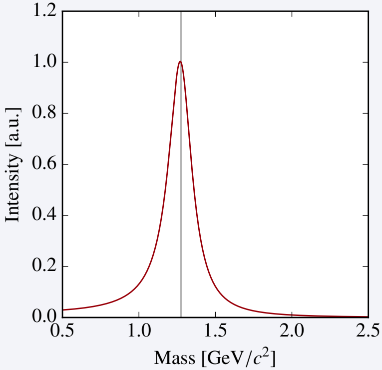

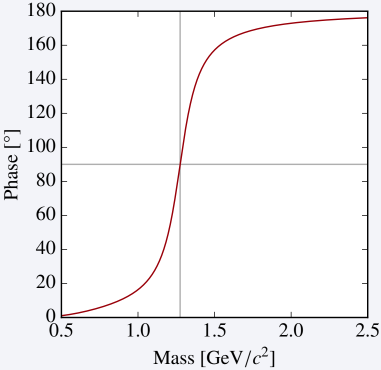

PWA $\pi^-\pi^-\pi^+$ Final State: Extraction of Resonances

[arXiv:1802.05913]

Ansatz for resonance model

$$\mathcal{T}_i(m_{3\pi}, t') \propto \sum_j \overbrace{\mathcal{C}_i^j(t')\, \mathcal{D}_j(m_{3\pi}, t'; \zeta_j)}^{\text{wave components}}$$

- Dynamical amplitudes $\mathcal{D}_j(m_{3\pi}, t'; \zeta_j)$
  - For resonances: Breit-Wigner amplitudes
  - For non-resonant components: (real-valued) empirical parametrizations
  - "Shape parameters" ζ_j
- "Coupling amplitudes" $\mathcal{C}_i^j(t')$
  - Strengths and phases of wave components
- Determine $\{\zeta_j\}$ and $\{\mathcal{C}_i^j(t')\}$ by χ^2-fit to PWA result

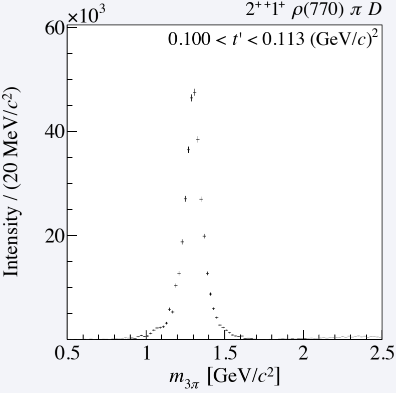

PWA $\pi^-\pi^-\pi^+$ Final State: Extraction of Resonances

[arXiv:1802.05913]

Ansatz for resonance model

$$\mathcal{T}_i(m_{3\pi}, t') \propto \underbrace{\sum_j}_{\text{wave components}} \mathcal{C}_i^j(t')\, \mathcal{D}_j(m_{3\pi}, t'; \zeta_j)$$

- Dynamical amplitudes $\mathcal{D}_j(m_{3\pi}, t'; \zeta_j)$
  - For resonances: Breit-Wigner amplitudes
  - For non-resonant components: (real-valued) empirical parametrizations
  - "Shape parameters" ζ_j
- "Coupling amplitudes" $\mathcal{C}_i^j(t')$
  - Strengths and phases of wave components
- Determine $\{\zeta_j\}$ and $\{\mathcal{C}_i^j(t')\}$ by χ^2-fit to PWA result

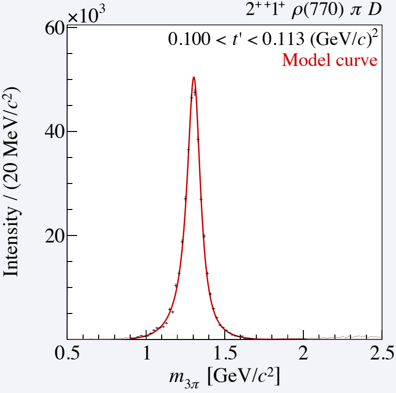

PWA $\pi^-\pi^-\pi^+$ Final State: Extraction of Resonances

[arXiv:1802.05913]

Ansatz for resonance model

$$\mathcal{T}_i(m_{3\pi}, t') \propto \sum_j^{\text{wave components}} \mathcal{C}_i^j(t')\, \mathcal{D}_j(m_{3\pi}, t'; \zeta_j)$$

- Dynamical amplitudes $\mathcal{D}_j(m_{3\pi}, t'; \zeta_j)$
  - For resonances: Breit-Wigner amplitudes
  - For non-resonant components: (real-valued) empirical parametrizations
  - "Shape parameters" ζ_j
- "Coupling amplitudes" $\mathcal{C}_i^j(t')$
  - Strengths and phases of wave components
- Determine $\{\zeta_j\}$ and $\{\mathcal{C}_i^j(t')\}$ by χ^2-fit to PWA result

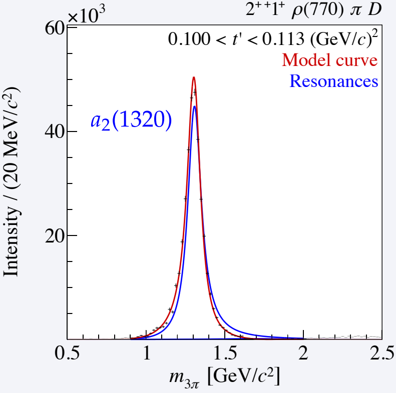

PWA $\pi^-\pi^-\pi^+$ Final State: Extraction of Resonances

[arXiv:1802.05913]

Ansatz for resonance model

$$\mathcal{T}_i(m_{3\pi}, t') \propto \sum_j \overbrace{\mathcal{C}_i^j(t')\,\mathcal{D}_j(m_{3\pi}, t'; \zeta_j)}^{\text{wave components}}$$

- Dynamical amplitudes $\mathcal{D}_j(m_{3\pi}, t'; \zeta_j)$
  - For resonances: Breit-Wigner amplitudes
  - For non-resonant components: (real-valued) empirical parametrizations
  - "Shape parameters" ζ_j
- "Coupling amplitudes" $\mathcal{C}_i^j(t')$
  - Strengths and phases of wave components
- Determine $\{\zeta_j\}$ and $\{\mathcal{C}_i^j(t')\}$ by χ^2-fit to PWA result

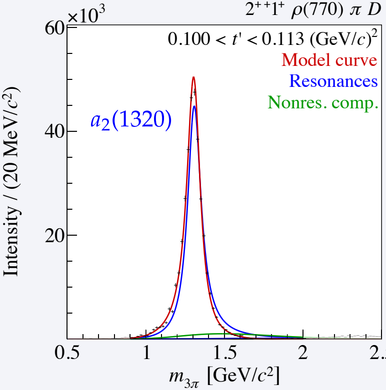

PWA $\pi^-\pi^-\pi^+$ Final State: Extraction of Resonances

[arXiv:1802.05913]

Ansatz for resonance model

$$\mathcal{T}_i(m_{3\pi}, t') \propto \underbrace{\sum_j}_{\text{wave components}} \mathcal{C}_i^j(t')\, \mathcal{D}_j(m_{3\pi}, t'; \zeta_j)$$

- Dynamical amplitudes $\mathcal{D}_j(m_{3\pi}, t'; \zeta_j)$
  - For resonances: Breit-Wigner amplitudes
  - For non-resonant components: (real-valued) empirical parametrizations
  - "Shape parameters" ζ_j
- "Coupling amplitudes" $\mathcal{C}_i^j(t')$
  - Strengths and phases of wave components
- Determine $\{\zeta_j\}$ and $\{\mathcal{C}_i^j(t')\}$ by χ^2-fit to PWA result

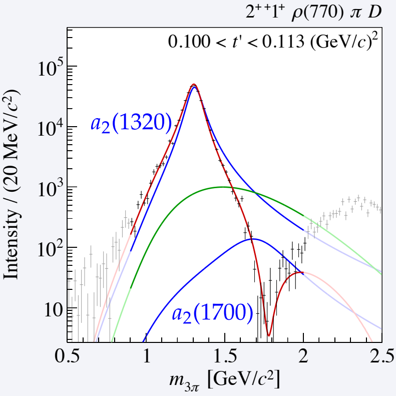

PWA $\pi^-\pi^-\pi^+$ Final State: Extraction of Resonances

[arXiv:1802.05913]

Ansatz for resonance model

$$\mathcal{T}_i(m_{3\pi}, t') \propto \overbrace{\sum_j}^{\text{wave components}} \mathcal{C}_i^j(t')\, \mathcal{D}_j(m_{3\pi}, t'; \zeta_j)$$

- Dynamical amplitudes $\mathcal{D}_j(m_{3\pi}, t'; \zeta_j)$
  - For resonances: Breit-Wigner amplitudes
  - For non-resonant components: (real-valued) empirical parametrizations
  - "Shape parameters" ζ_j
- "Coupling amplitudes" $\mathcal{C}_i^j(t')$
  - Strengths and phases of wave components
- Determine $\{\zeta_j\}$ and $\{\mathcal{C}_i^j(t')\}$ by χ^2-fit to PWA result

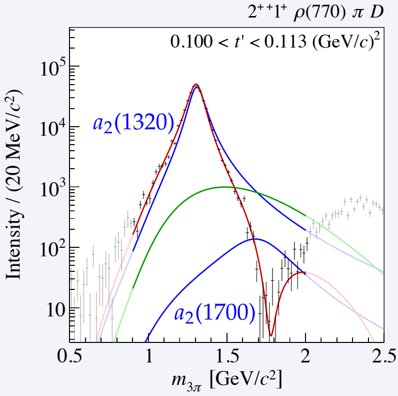

Ansatz for resonance model

$$\mathcal{T}_i(m_{3\pi}, t') \propto \overbrace{\sum_j}^{\text{wave components}} \mathcal{C}_i^j(t')\, \mathcal{D}_j(m_{3\pi}, t'; \zeta_j)$$

- Dynamical amplitudes $\mathcal{D}_j(m_{3\pi}, t'; \zeta_j)$
  - For resonances: Breit-Wigner amplitudes
  - For non-resonant components: (real-valued) empirical parametrizations
  - "Shape parameters" ζ_j
- "Coupling amplitudes" $\mathcal{C}_i^j(t')$
  - Strengths and phases of wave components
- Determine $\{\zeta_j\}$ and $\{\mathcal{C}_i^j(t')\}$ by χ^2-fit to PWA result

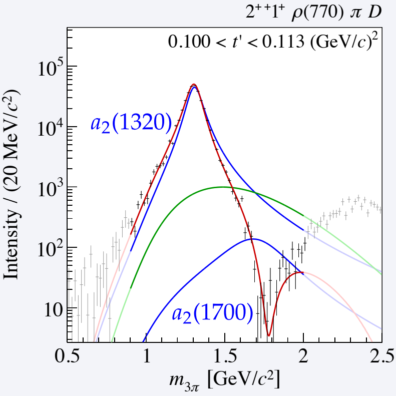

PWA $\pi^-\pi^-\pi^+$ Final State: Extraction of Resonances

[arXiv:1802.05913]

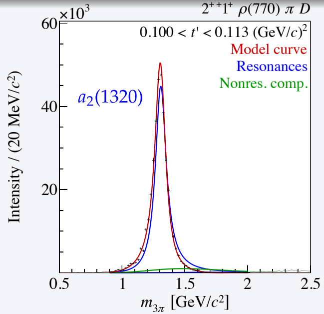

- Exploit phase information to extract resonances
- Only relative phases can be measured
- Fit several waves simultaneously
- Select waves with clear resonance signals

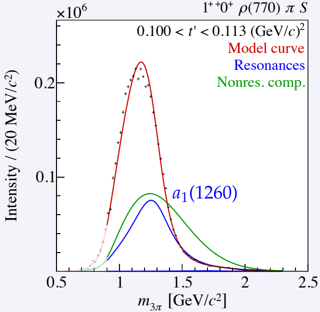

PWA $\pi^-\pi^-\pi^+$ Final State: Extraction of Resonances

[arXiv:1802.05913]

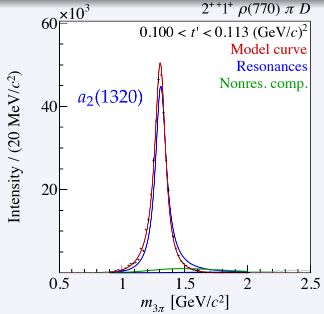

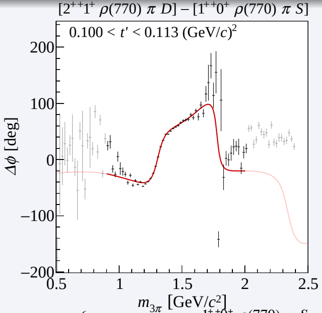

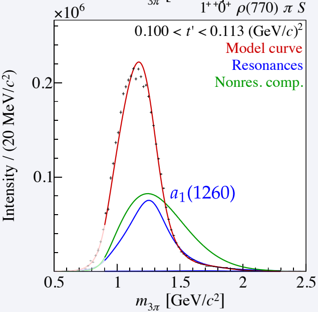

- Exploit phase information to extract resonances
- Only relative phases can be measured
- Fit several waves simultaneously
- Select waves with clear resonance signals

PWA $\pi^-\pi^-\pi^+$ Final State: Extraction of Resonances

[arXiv:1802.05913]

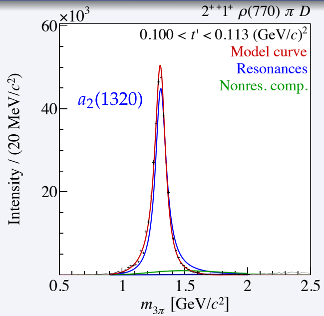

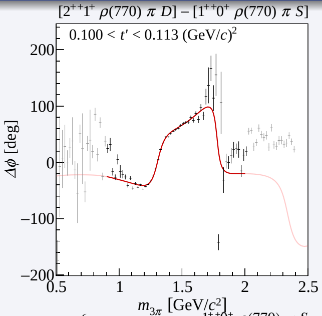

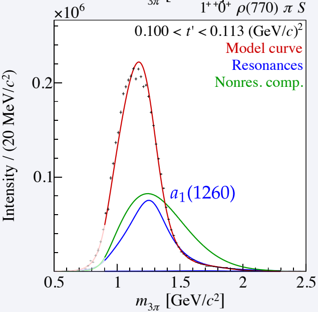

- Exploit phase information to extract resonances
- Only relative phases can be measured
- Fit several waves simultaneously
- Select waves with clear resonance signals

Resonance-Model Fit of $\pi^-\pi^-\pi^+$ Data

[arXiv:1802.05913]

- Selected 14 waves with clear resonance signals
  - Represent ca. 60 % of total intensity
  - Most comprehensive analysis of this type so far
- Data described by 11 resonances + one non-resonant component in each wave
- Fit 11 t' bins simultaneously
- Same resonance parameters in all t' bins
- Large fit
  - 722 real-valued fit parameters constraint by ca. 76 500 data points
  - Only 51 shape parameters
- Model not perfect
  - Tensions with data
  - Multimodal behavior of χ^2 function
  - Result depends on choice of start parameters
  - Perform 1000 fit attempts
- Expensive: one fit result $\approx$ 30 000 CPUh

Resonance-Model Fit of $\pi^-\pi^-\pi^+$ Data

[arXiv:1802.05913]

- Selected 14 waves with clear resonance signals
  - Represent ca. 60 % of total intensity
  - Most comprehensive analysis of this type so far
- Data described by 11 resonances + one non-resonant component in each wave
- Fit 11 t' bins simultaneously
- Same resonance parameters in all t' bins
- Large fit
  - 722 real-valued fit parameters constraint by ca. 76 500 data points
  - Only 51 shape parameters
- Model not perfect
  - Tensions with data
  - Multimodal behavior of χ^2 function
  - Result depends on choice of start parameters
  - Perform 1000 fit attempts
- Expensive: one fit result $\approx$ 30 000 CPUh

Resonance-Model Fit of $\pi^-\pi^-\pi^+$ Data

[arXiv:1802.05913]

- Selected 14 waves with clear resonance signals
  - Represent ca. 60 % of total intensity
  - Most comprehensive analysis of this type so far
- Data described by 11 resonances + one non-resonant component in each wave
- Fit 11 t' bins simultaneously
- Same resonance parameters in all t' bins
- Large fit
  - 722 real-valued fit parameters constraint by ca. 76 500 data points
  - Only 51 shape parameters
- Model not perfect
  - Tensions with data
  - Multimodal behavior of χ^2 function
  - Result depends on choice of start parameters
  - Perform 1000 fit attempts
- Expensive: one fit result $\approx$ 30 000 CPUh

Resonance-Model Fit of $\pi^-\pi^-\pi^+$ Data

[arXiv:1802.05913]

- Selected 14 waves with clear resonance signals
  - Represent ca. 60 % of total intensity
  - Most comprehensive analysis of this type so far
- Data described by 11 resonances + one non-resonant component in each wave
- Fit 11 t' bins simultaneously
- Same resonance parameters in all t' bins
- Large fit
  - 722 real-valued fit parameters constraint by ca. 76 500 data points
  - Only 51 shape parameters
- Model not perfect
  - Tensions with data
  - Multimodal behavior of χ^2 function
  - Result depends on choice of start parameters
  - Perform 1000 fit attempts
- Expensive: one fit result $\approx$ 30 000 CPUh

Resonance-Model Fit of $\pi^-\pi^-\pi^+$ Data

[arXiv:1802.05913]

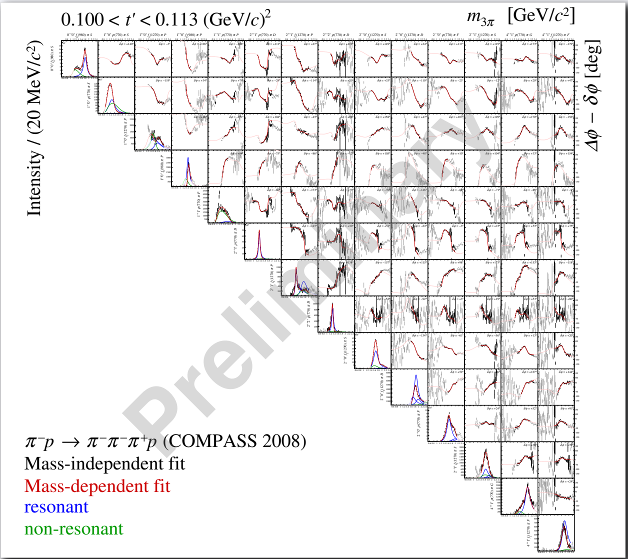

Resonance-Model Fit of $\pi^-\pi^-\pi^+$ Data

[arXiv:1802.05913]

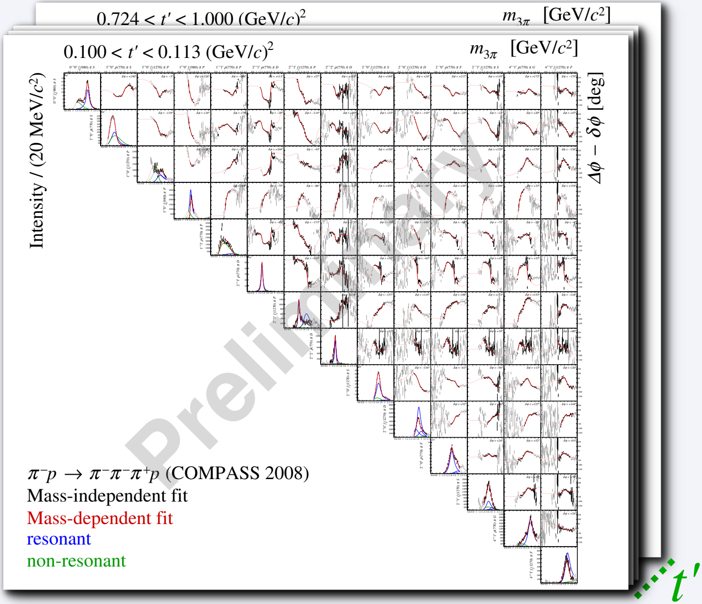

t'-resolved Resonance-Model Fit

$2^{++}\,1^{+}\,\rho(770)\,\pi\,D$

- $a_2(1320)$: shape of peak does not depend on t'
- $a_2(1700)$: complicated t'-dependent interference with other wave components

t' information helps disentangling resonant from non-resonant components

low t'

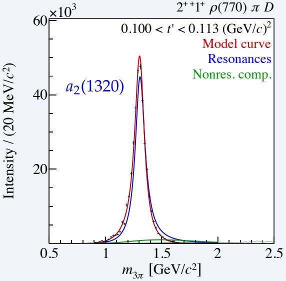

high t'

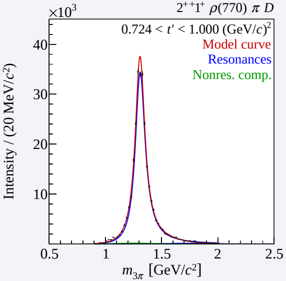

t'-resolved Resonance-Model Fit

[arXiv:1802.05913]

$2^{++}\,1^{+}\,\rho(770)\,\pi\,D$

- $a_2(1320)$: shape of peak does not depend on t'
- $a_2(1700)$: complicated t'-dependent interference with other wave components

t' information helps disentangling resonant from non-resonant components

low t'

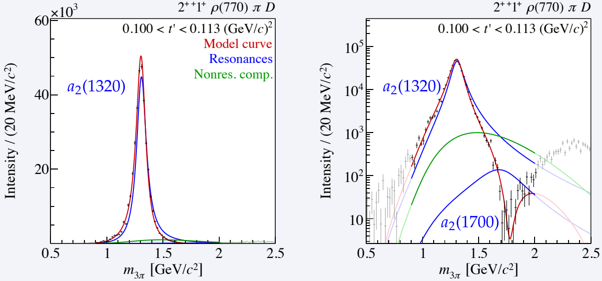

high t'

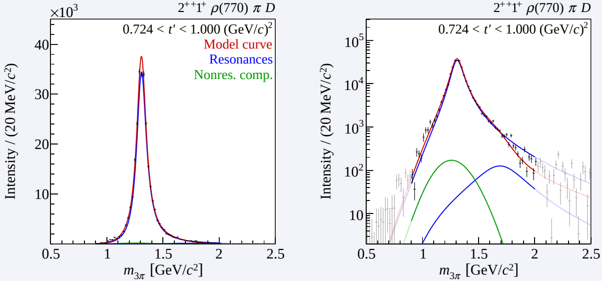

t'-resolved Resonance-Model Fit

$2^{++}\,1^{+}\,\rho(770)\,\pi\,D$

- $a_2(1320)$: shape of peak does not depend on t'
- $a_2(1700)$: complicated t'-dependent interference with other wave components

t' information helps disentangling resonant from non-resonant components

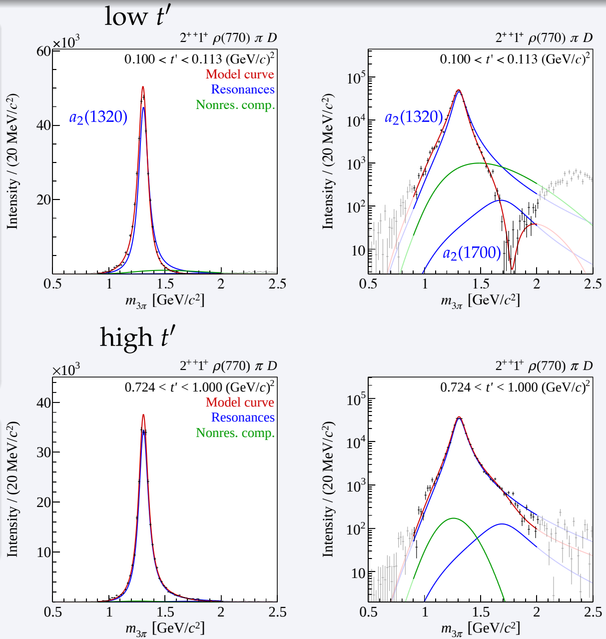

t'-resolved Resonance-Model Fit

$2^{++}\, 1^{+}\, \rho(770)\, \pi\, D$

- $a_2(1320)$: shape of peak does not depend on t'
- $a_2(1700)$: complicated t'-dependent interference with other wave components

Resonance parameters

- $a_2(1320)$
  $$m_0 = (1314.5\,^{+4.0}_{-3.3})\ \mathrm{MeV}/c^2$$
  $$\Gamma_0 = (106.6\,^{+3.4}_{-7.0})\ \mathrm{MeV}/c^2$$
- $a_2(1700)$
  $$m_0 = (1681\,^{+22}_{-35})\ \mathrm{MeV}/c^2$$
  $$\Gamma_0 = (436\,^{+20}_{-16})\ \mathrm{MeV}/c^2$$

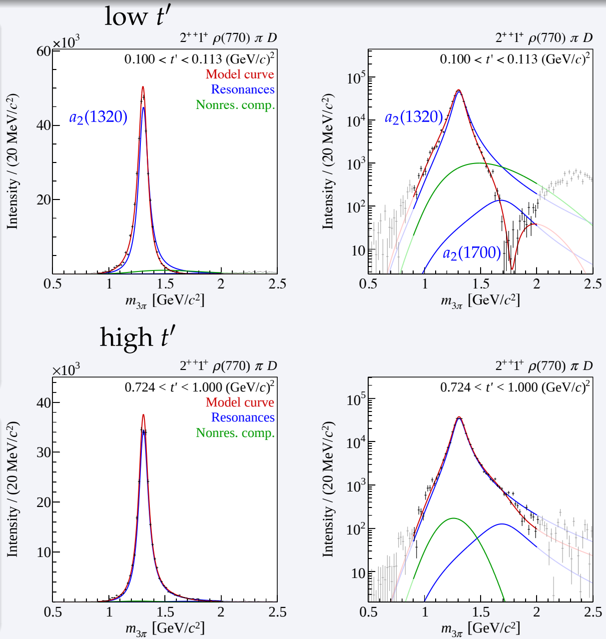

$2^{++}\,1^{+}\,\rho(770)\,\pi\,D$ Components: t' Spectra

[arXiv:1802.05913]

- For each t' bin: integrate intensity of wave components over fitted $m_{3\pi}$ range
- Fit t' spectrum with simple model: $\mathcal{I}_j(t') = A_j \cdot (t')^{|M|} \cdot e^{-b_j\,t'}$
  - Slope parameter b_j

$a_2(1320)$ | $a_2(1700)$ | non-resonant

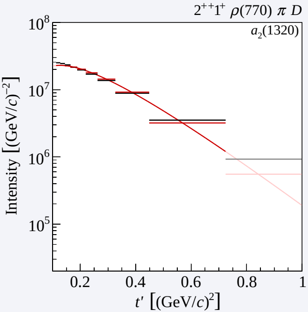

$b = (7.9 \pm 0.5)\ (\mathrm{GeV}/c)^{-2}$ | $b = (7.3\,^{+2.4}_{-0.9})\ (\mathrm{GeV}/c)^{-2}$ | $b = (13.6\,^{+0.4}_{-1.8})\ (\mathrm{GeV}/c)^{-2}$

$2^{++}1^{+}\,\rho(770)\,\pi\,D$ Components: t' Spectra

[arXiv:1802.05913]

- For each t' bin: integrate intensity of wave components over fitted $m_{3\pi}$ range
- Fit t' spectrum with simple model: $\mathcal{I}_j(t') = A_j \cdot (t')^{|M|} \cdot e^{-b_j\,t'}$
  - Slope parameter b_j

$a_2(1320)$

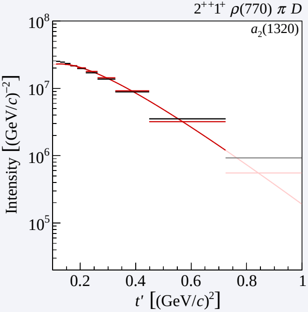

$b = (7.9 \pm 0.5)\,(\mathrm{GeV}/c)^{-2}$

$a_2(1700)$

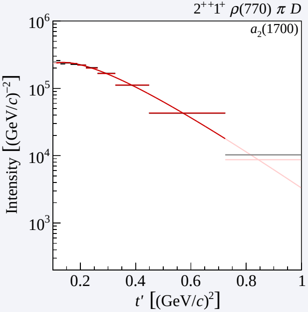

$b = (7.3\,^{+2.4}_{-0.9})\,(\mathrm{GeV}/c)^{-2}$

non-resonant

$b = (13.6\,^{+0.4}_{-1.8})\,(\mathrm{GeV}/c)^{-2}$

$2^{++}1^{+}\,\rho(770)\,\pi\,D$ Components: t' Spectra

[arXiv:1802.05913]

- For each t' bin: integrate intensity of wave components over fitted $m_{3\pi}$ range
- Fit t' spectrum with simple model: $\mathcal{I}_j(t') = A_j \cdot (t')^{|M|} \cdot e^{-b_j t'}$
  - Slope parameter b_j

$a_2(1320)$

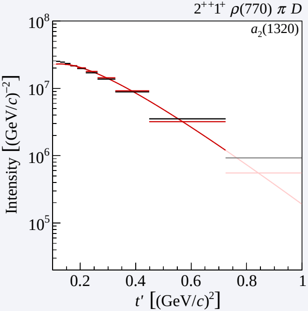

$b = (7.9 \pm 0.5)\ (\mathrm{GeV}/c)^{-2}$

$a_2(1700)$

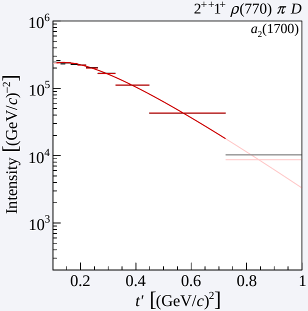

$b = (7.3\,^{+2.4}_{-0.9})\ (\mathrm{GeV}/c)^{-2}$

non-resonant

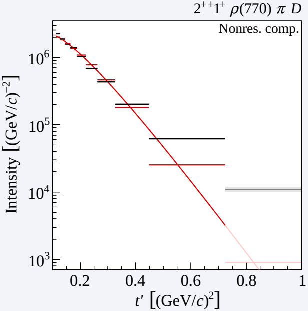

$b = (13.6\,^{+0.4}_{-1.8})\ (\mathrm{GeV}/c)^{-2}$

Comparison with COMPASS $\eta\pi$ Data

Diffractively produced $\eta\pi^-$

C. Adolph *et al.*, PLB **740** (2015) 303

- Clear $a_2(1320)$ peak
- Dominant D-wave

Reanalysis with improved resonance model

A. Jackura *et al.*, PLB **779** (2018) 464

- Analytical model based on S-matrix principles
  - Developed by JPAC
  - Includes effects from final-state interactions
- Process-independent pole positions of resonances
  - 2 poles: $a_2(1320)$ and $a_2(1700)$

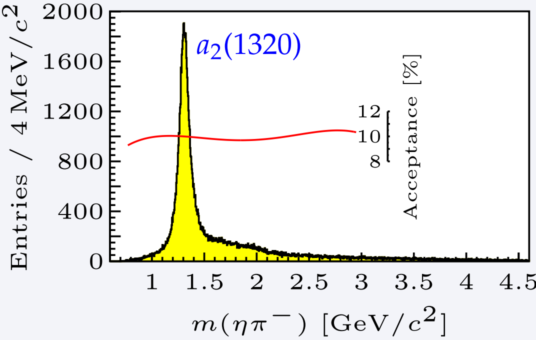

Comparison with COMPASS $\eta\pi$ Data

Diffractively produced $\eta\pi^-$

C. Adolph *et al.*, PLB **740** (2015) 303

- Clear $a_2(1320)$ peak
- Dominant D-wave

Reanalysis with improved resonance model

A. Jackura *et al.*, PLB **779** (2018) 464

- Analytical model based on S-matrix principles
  - Developed by JPAC
  - Includes effects from final-state interactions
- Process-independent pole positions of resonances
  - 2 poles: $a_2(1320)$ and $a_2(1700)$

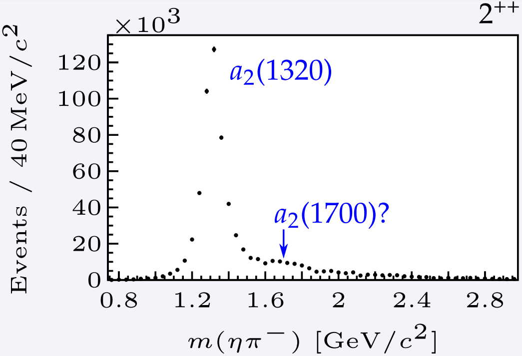

Comparison with COMPASS $\eta\pi$ Data

Diffractively produced $\eta\pi^-$

C. Adolph *et al.*, PLB **740** (2015) 303

- Clear $a_2(1320)$ peak
- Dominant D-wave

Reanalysis with improved resonance model

A. Jackura *et al.*, PLB **779** (2018) 464

- Analytical model based on S-matrix principles
  - Developed by JPAC
  - Includes effects from final-state interactions
- Process-independent pole positions of resonances
  - 2 poles: $a_2(1320)$ and $a_2(1700)$

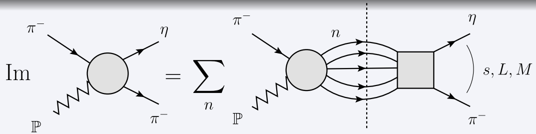

Comparison with COMPASS $\eta\pi$ Data

Diffractively produced $\eta\pi^-$

C. Adolph *et al.*, PLB **740** (2015) 303

- Clear $a_2(1320)$ peak
- Dominant D-wave

Reanalysis with improved resonance model

A. Jackura *et al.*, PLB **779** (2018) 464

- Analytical model based on S-matrix principles
  - Developed by JPAC
  - Includes effects from final-state interactions
- Process-independent pole positions of resonances
  - 2 poles: $a_2(1320)$ and $a_2(1700)$

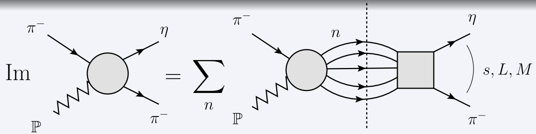

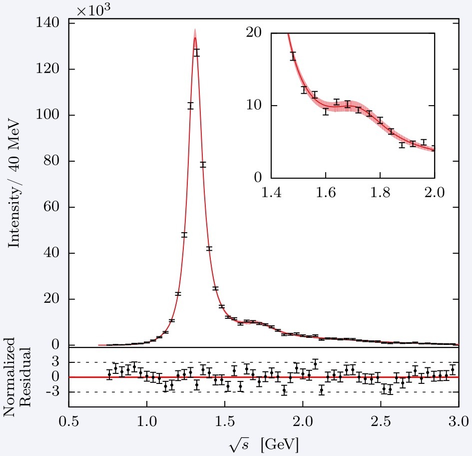

Comparison with COMPASS $\eta\pi$ Data

$a_2(1320)$ parameters in agreement

From $\pi^-\pi^-\pi^+$ analysis:

$$m_0 = (1314.5\,^{+4.0}_{-3.3})\ \mathrm{MeV}/c^2$$

$$\Gamma_0 = (106.6\,^{+3.4}_{-7.0})\ \mathrm{MeV}/c^2$$

[arXiv:1802.05913]

From $\eta\pi$ analysis:

$$m_0 = (1307 \pm 1_{\,\mathrm{stat.}} \pm 6_{\,\mathrm{sys.}})\ \mathrm{MeV}/c^2$$

$$\Gamma_0 = (112 \pm 1_{\,\mathrm{stat.}} \pm 8_{\,\mathrm{sys.}})\ \mathrm{MeV}/c^2$$

A. Jackura *et al.*, PLB **779** (2018) 464

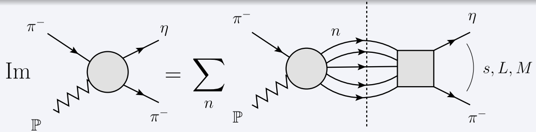

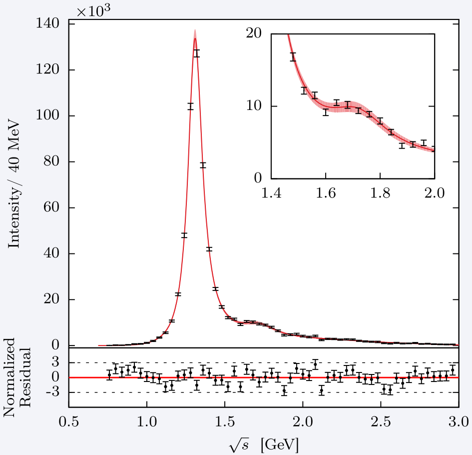

Comparison with COMPASS $\eta\pi$ Data

$a_2(1700)$ parameters

From $\pi^-\pi^-\pi^+$ analysis:

$$m_0 = (1681\,^{+22}_{-35})\ \mathrm{MeV}/c^2$$
$$\Gamma_0 = (436\,^{+20}_{-16})\ \mathrm{MeV}/c^2$$

[arXiv:1802.05913]

From $\eta\pi$ analysis:

$$m_0 = (1720 \pm 10_{\,\text{stat.}} \pm 60_{\,\text{sys.}})\ \mathrm{MeV}/c^2$$
$$\Gamma_0 = (280 \pm 10_{\,\text{stat.}} \pm 70_{\,\text{sys.}})\ \mathrm{MeV}/c^2$$

A. Jackura *et al.*, PLB **779** (2018) 464

- $a_2(1700)$ masses in agreement
- Breit-Wigner width from $\pi^-\pi^-\pi^+$ analysis $156\ \mathrm{MeV}/c^2$ larger

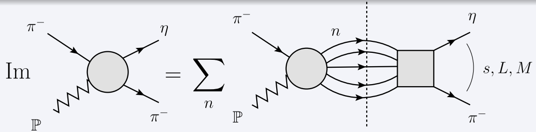

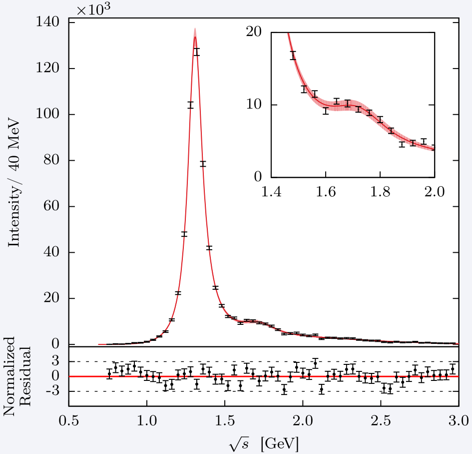

Spin-exotic $1^{-+}1^{+}\rho(770)\,\pi\,P$ Wave

- Shape of intensity distribution changes dramatically with t'
  - Low t': mostly non-resonant
  - High t': mostly $\pi_1(1600)$
- Large model dependence

Resonance parameters

- $\pi_1(1600)$
  $m_0 = (1600\,^{+110}_{-60})\ \mathrm{MeV}/c^2$
  $\Gamma_0 = (580\,^{+100}_{-230})\ \mathrm{MeV}/c^2$
- PDG average
  $m_0 = (1662\,^{+8}_{-9})\ \mathrm{MeV}/c^2$
  $\Gamma_0 = (241 \pm 40)\ \mathrm{MeV}/c^2$

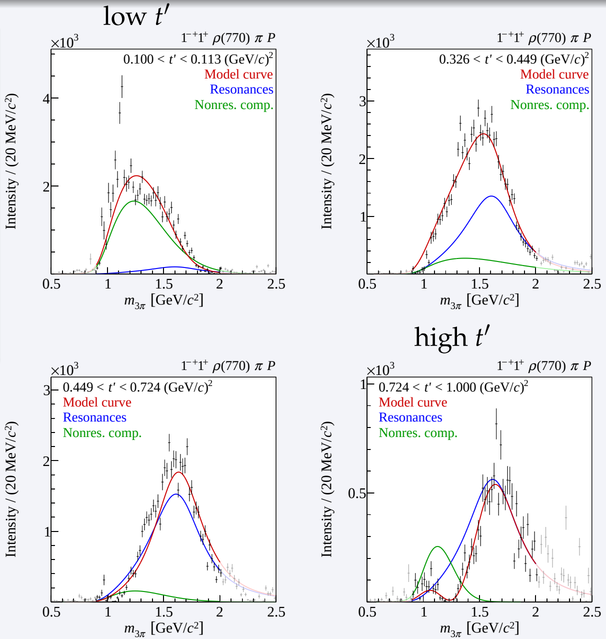

Spin-exotic $1^{-+} 1^{+} \rho(770)\, \pi\, P$ Wave

[arXiv:1802.05913]

- Shape of intensity distribution changes dramatically with t'
  - Low t': mostly non-resonant
  - High t': mostly $\pi_1(1600)$
- Large model dependence

Resonance parameters

- $\pi_1(1600)$

  $m_0 = (1600\,^{+110}_{-60})\ \mathrm{MeV}/c^2$

  $\Gamma_0 = (580\,^{+100}_{-230})\ \mathrm{MeV}/c^2$
- PDG average

  $m_0 = (1662\,^{+8}_{-9})\ \mathrm{MeV}/c^2$

  $\Gamma_0 = (241 \pm 40)\ \mathrm{MeV}/c^2$

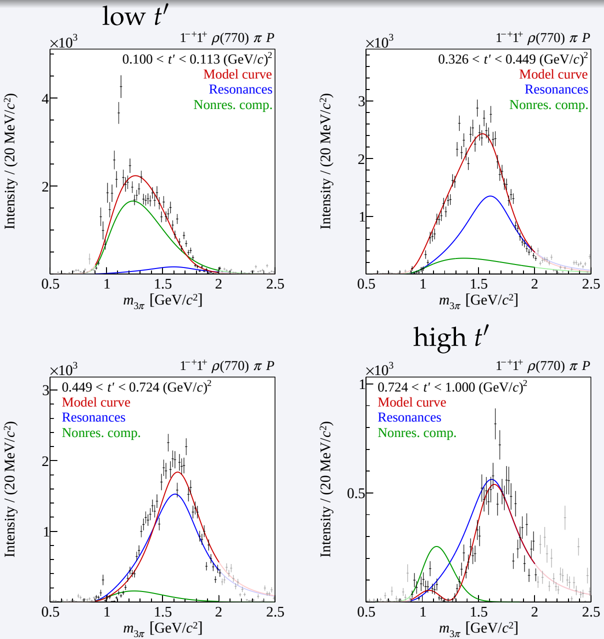

Spin-exotic $1^{-+}1^{+}\rho(770)\,\pi\,P$ Wave

- Data at high t' cannot be described without $\pi_1(1600)$ component (dashed curves)

low t' | high t' | phase at high t'

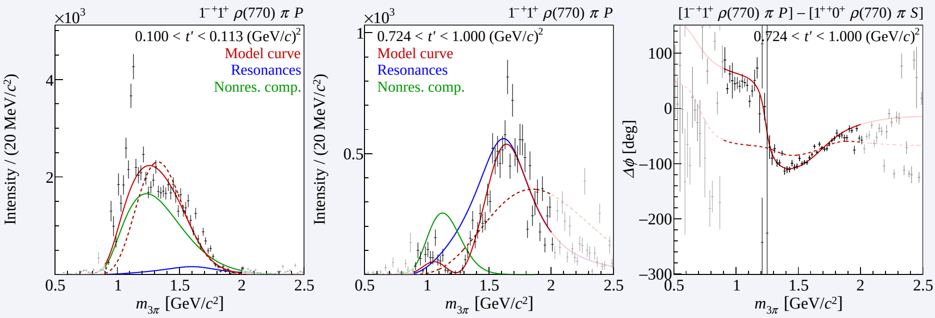

Model for Non-resonant Component

[arXiv:1802.05913]

Purely empirical parametrization for non-resonant components

$$\mathcal{D}_j^{\mathrm{NR}}(m_{3\pi}, t'; b, c_0, c_1, c_2) = \left[\frac{m_{3\pi} - m_{\mathrm{thr}}}{m_{\mathrm{norm}}}\right]^b e^{-(c_0 + c_1\, t' + c_2\, t'^2)\, q^2}$$

- $m_{\mathrm{thr}} = 0.5\,\mathrm{GeV}/c^2$ and $m_{\mathrm{norm}} = 1\,\mathrm{GeV}/c^2$
- q is breakup momentum of $X \to \text{isobar} + \pi$

Deck effect

- MC pseudodata generated according to model of Deck amplitude

based on ACCMOR, NPB **182** (1981) 269

- Use partial-wave projections as non-resonant components

Model for Non-resonant Component

[arXiv:1802.05913]

Purely empirical parametrization for non-resonant components

$$\mathcal{D}_j^{\mathrm{NR}}(m_{3\pi}, t'; b, c_0, c_1, c_2) = \left[\frac{m_{3\pi} - m_{\mathrm{thr}}}{m_{\mathrm{norm}}}\right]^b e^{-(c_0 + c_1\, t' + c_2\, t'^2)\, q^2}$$

- $m_{\mathrm{thr}} = 0.5\,\mathrm{GeV}/c^2$ and $m_{\mathrm{norm}} = 1\,\mathrm{GeV}/c^2$
- q is breakup momentum of $X \to \text{isobar} + \pi$

Deck effect

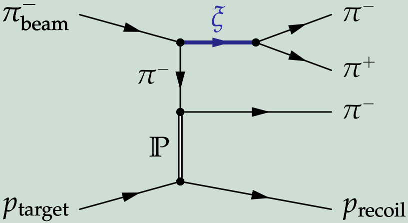

- MC pseudodata generated according to model of Deck amplitude

  based on ACCMOR, NPB **182** (1981) 269

- Use partial-wave projections as non-resonant components

Model for Non-resonant Component

- *Dashed curves:* partial-wave projection of Deck model used as non-resonant component
  - Good description of data
  - Higher $\pi_1(1600)$ yield at low t'

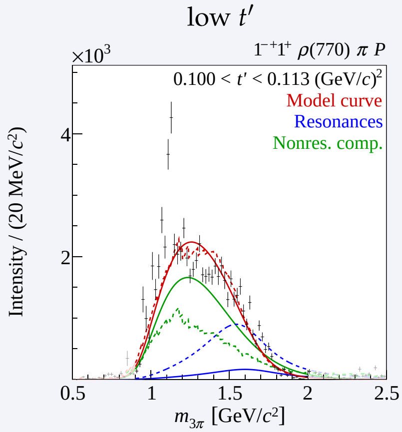

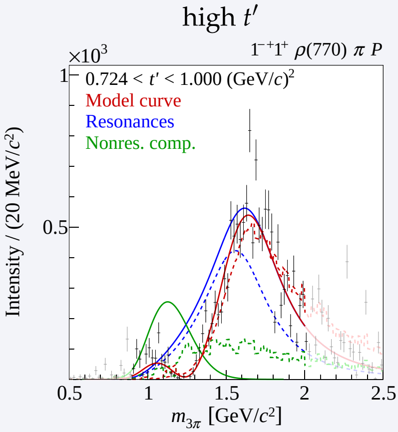

$1^{++}\,0^{+}\,f_0(980)\,\pi\,P$ Wave: A New $a_1(1420)$ Meson?

C. Adolph *et al.*, PRL **115** (2015) 082001 and *[arXiv:1802.05913]*

- **Unexpected peak around 1.4 GeV/c^2**
- Small intensity: only 0.3 % relative contribution
- Peak and phase motion well described by Breit-Wigner amplitude

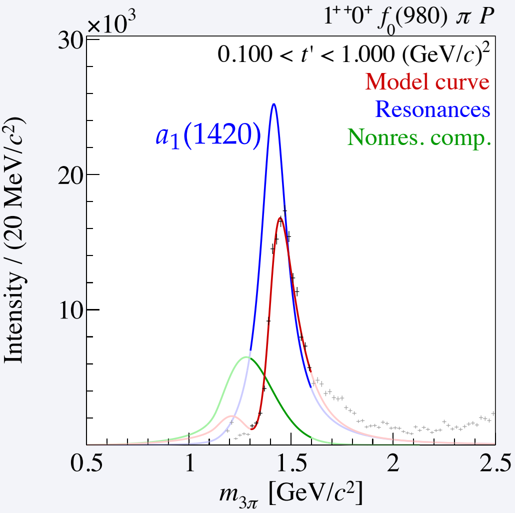

Resonance parameters

- $a_1(1420)$
  $m_0 = (1411\,^{+4}_{-5})$ MeV/c^2
  $\Gamma_0 = (161\,^{+11}_{-14})$ MeV/c^2
- Suspiciously close to KK^* threshold

$1^{++}\,0^+\,f_0(980)\,\pi\,P$ Wave: A New $a_1(1420)$ Meson?

C. Adolph *et al.*, PRL **115** (2015) 082001 and *[arXiv:1802.05913]*

- **Unexpected peak around 1.4 GeV/c^2**
- Small intensity: only 0.3 % relative contribution
- Peak and phase motion well described by Breit-Wigner amplitude

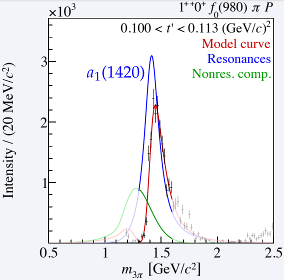

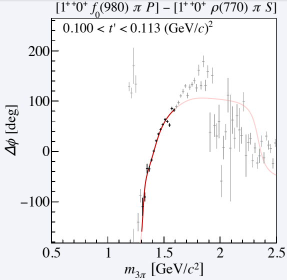

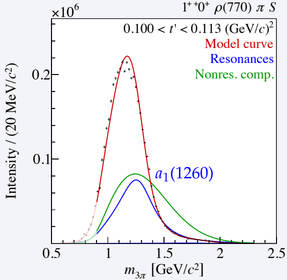

Resonance parameters

- $a_1(1420)$

  $m_0 = (1411\,^{+4}_{-5})\ \mathrm{MeV}/c^2$

  $\Gamma_0 = (161\,^{+11}_{-14})\ \mathrm{MeV}/c^2$
- Suspiciously close to KK^* threshold

$1^{++}0^{+}\,f_0(980)\,\pi\,P$ Wave: A New $a_1(1420)$ Meson?

C. Adolph *et al.*, PRL **115** (2015) 082001 and *[arXiv:1802.05913]*

- **Unexpected peak around 1.4 GeV/c^2**
- Small intensity: only 0.3 % relative contribution
- Peak and phase motion well described by Breit-Wigner amplitude

Resonance parameters

- $a_1(1420)$
  $$m_0 = (1411\,^{+4}_{-5})\ \text{MeV}/c^2$$
  $$\Gamma_0 = (161\,^{+11}_{-14})\ \text{MeV}/c^2$$
- Suspiciously close to KK^* threshold

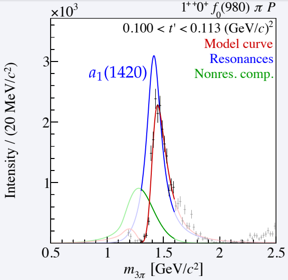

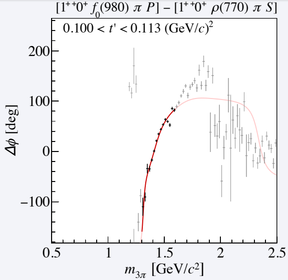

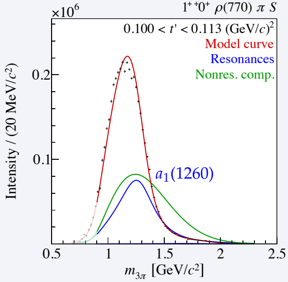

What is the Nature of the $a_1(1420)$?

Proposed Explanations without additional Resonance

Effect in production of $a_1(1260)$?

- Two-channel unitarized Deck amplitude + direct $a_1(1260)$ production

Basdevant and Berger, PRL **114** (2015) 192001 and *[arXiv:1501.04643]*

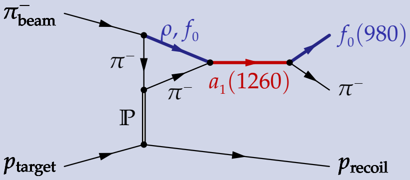

- Phase motion around $a_1(1260)$ instead around $1.4\,\mathrm{GeV}/c^2$

Effect in production of $a_1(1260)$?

- Two-channel unitarized Deck amplitude + direct $a_1(1260)$ production
  Basdevant and Berger, PRL **114** (2015) 192001 and *[arXiv:1501.04643]*

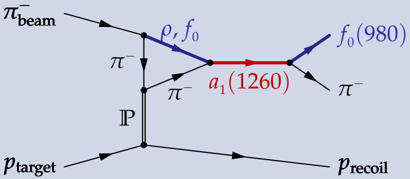

- Phase motion around $a_1(1260)$ instead around $1.4\,\text{GeV}/c^2$

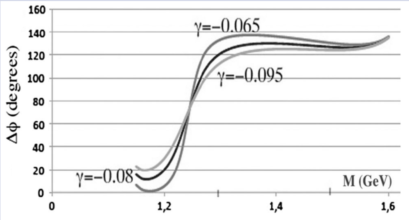

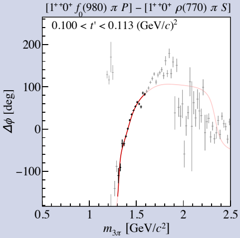

Effect in decay of $a_1(1260)$?

- Singularity in triangle diagram

Mikhasenko *et al.*, PRD **91** (2015) 094015
Aceti *et al.*, PRD **94** (2016) 096015

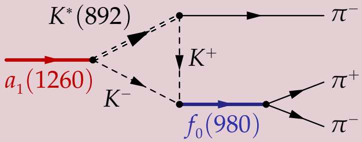

- Describes data equally well as Breit-Wigner amplitude

Effect in decay of $a_1(1260)$?

- Singularity in triangle diagram

Mikhasenko *et al.*, PRD **91** (2015) 094015
Aceti *et al.*, PRD **94** (2016) 096015

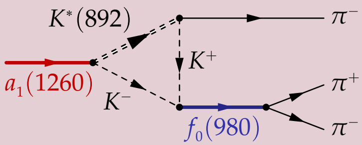

- Describes data equally well as Breit-Wigner amplitude

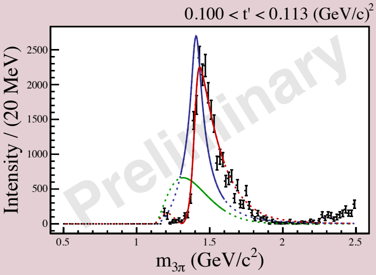

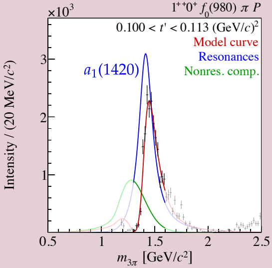

Summary: Parameters of a_J-like Resonances

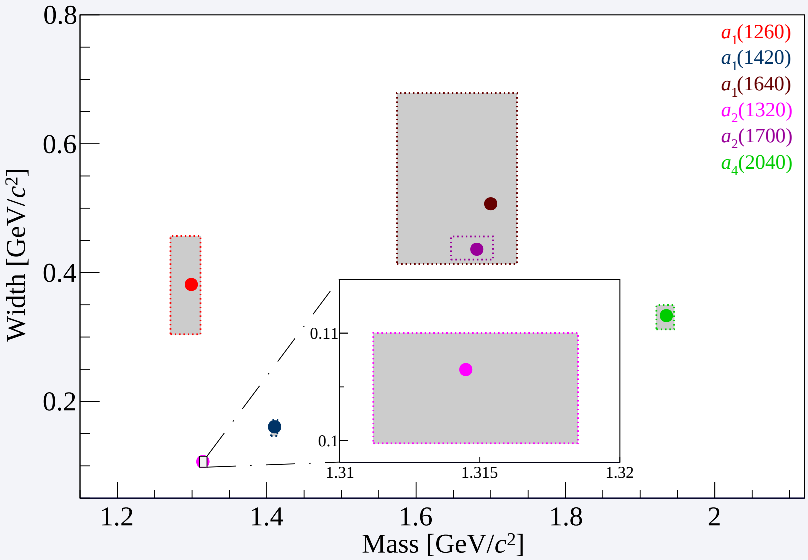

Resonance-Model Fit of $\pi^-\pi^-\pi^+$ Data

Summary: Parameters of π_J-like Resonances

[arXiv:1802.05913]

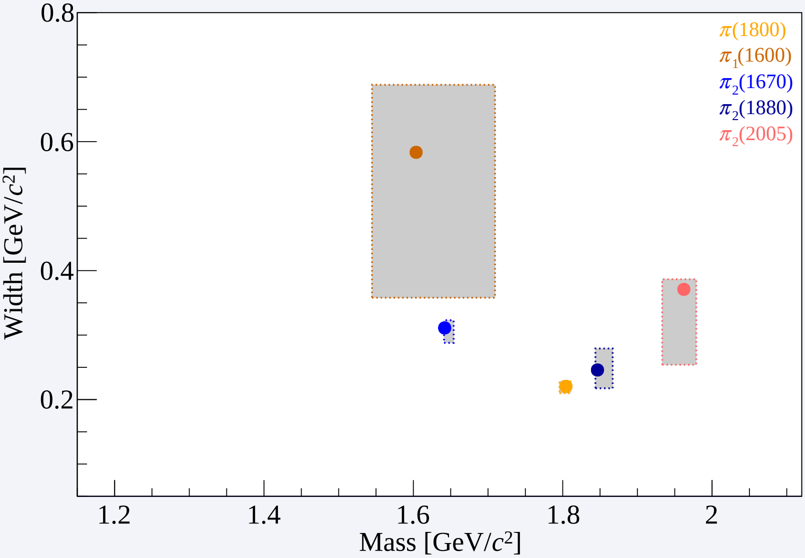

Conclusions and Outlook

Diffractively produced multi-body final states

- Ideal laboratory to study hadronic resonances and hadron dynamics

Large data sets allow us to employ novel analysis techniques

- *t'-resolved analysis:* better separation of resonant and non-resonant components

Non-resonant components play important role

- Limit accuracy of resonance parameters
- First studies based on Deck models are promising
- Tight collaboration with theorists to improve analysis model

Other ongoing analyses

- Pion diffraction into $\pi^-\eta, \pi^-\eta', \pi^-\pi^0\omega, \ldots$
- Kaon diffraction into $K^-\pi^+\pi^-, \ldots$

Conclusions and Outlook

Diffractively produced multi-body final states

- Ideal laboratory to study hadronic resonances and hadron dynamics

Large data sets allow us to employ **novel analysis techniques**

- *t'-resolved analysis:* better separation of resonant and non-resonant components

Non-resonant components play important role

- Limit accuracy of resonance parameters
- First studies based on Deck models are promising
- Tight collaboration with theorists to improve analysis model

Other ongoing analyses

- Pion diffraction into $\pi^-\eta, \pi^-\eta', \pi^-\pi^0\omega, \ldots$
- Kaon diffraction into $K^-\pi^+\pi^-, \ldots$

Conclusions and Outlook

Diffractively produced multi-body final states

- Ideal laboratory to study hadronic resonances and hadron dynamics

Large data sets allow us to employ **novel analysis techniques**

- *t'-resolved analysis:* better separation of resonant and non-resonant components

Non-resonant components play important role

- Limit accuracy of resonance parameters
- First studies based on Deck models are promising
- Tight collaboration with theorists to improve analysis model

Other ongoing analyses

- Pion diffraction into $\pi^-\eta$, $\pi^-\eta'$, $\pi^-\pi^0\omega$, ...
- Kaon diffraction into $K^-\pi^+\pi^-$, ...

Conclusions and Outlook

Diffractively produced multi-body final states

- Ideal laboratory to study hadronic resonances and hadron dynamics

Large data sets allow us to employ **novel analysis techniques**

- *t'-resolved analysis:* better separation of resonant and non-resonant components

Non-resonant components play important role

- Limit accuracy of resonance parameters
- First studies based on Deck models are promising
- Tight collaboration with theorists to improve analysis model

Other ongoing analyses

- Pion diffraction into $\pi^-\eta$, $\pi^-\eta'$, $\pi^-\pi^0\omega$, ...
- Kaon diffraction into $K^-\pi^+\pi^-$, ...

Outline

$1^{++}\,0^{+}\,\rho(770)\,\pi\,S$ Wave Components

[arXiv:1802.05913]

$a_1(1260)$

- Shape and position of peak changes significantly with t'
- Fair agreement of model with data
- Large non-resonant component
  - Large model dependence

Resonance parameters

- Our result

$$m_0 = (1299\,^{+12}_{-28})\ \mathrm{MeV}/c^2$$
$$\Gamma_0 = (380 \pm 80)\ \mathrm{MeV}/c^2$$

- PDG estimate

$$m_0 = (1230 \pm 40)\ \mathrm{MeV}/c^2$$
$$\Gamma_0 = 250\ \text{to}\ 600\ \mathrm{MeV}/c^2$$

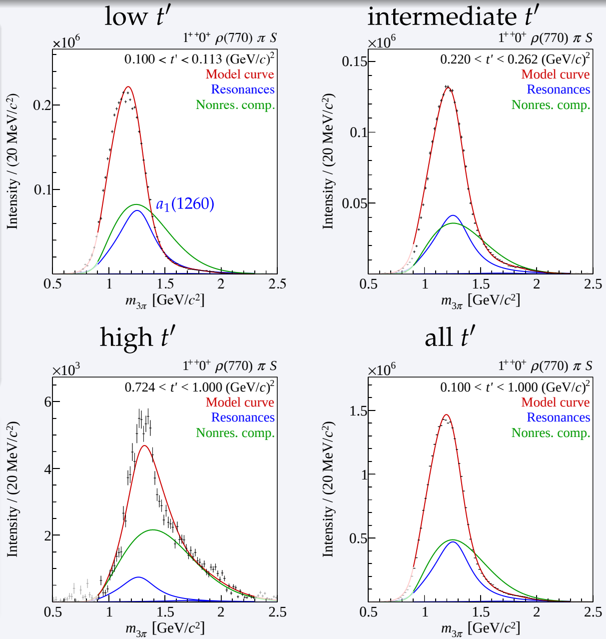

$1^{++}\,0^{+}\,\rho(770)\,\pi\,S$ Wave Components

[arXiv:1802.05913]

$a_1(1260)$

- Shape and position of peak changes significantly with t'
- Fair agreement of model with data
- Large non-resonant component
  - Large model dependence

Resonance parameters

- Our result

$$m_0 = (1299\,^{+12}_{-28})\,\mathrm{MeV}/c^2$$
$$\Gamma_0 = (380 \pm 80)\,\mathrm{MeV}/c^2$$

- PDG estimate

$$m_0 = (1230 \pm 40)\,\mathrm{MeV}/c^2$$
$$\Gamma_0 = 250 \text{ to } 600\,\mathrm{MeV}/c^2$$

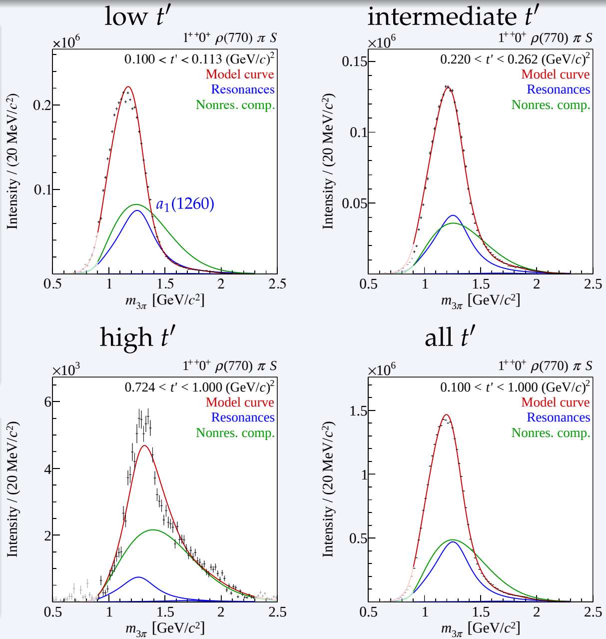

Model for Non-resonant Component

$1^{++}\,0^{+}\,\rho(770)\,\pi\,S$ Wave

- *Dashed curves:* partial-wave projection of Deck model used as non-resonant component
  - Good description of data
  - Different $a_1(1260)$ yields

low t'

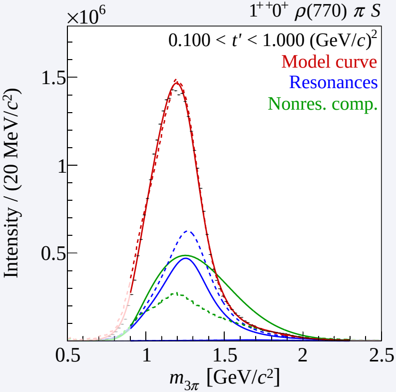

high t'

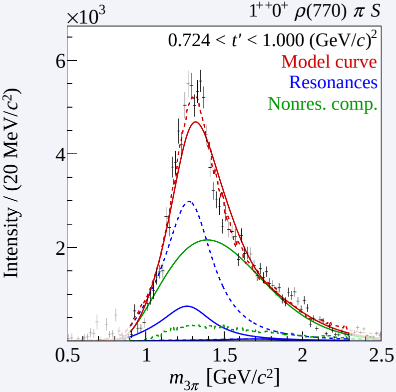

$1^{++}\,0^{+}\,\rho(770)\,\pi\,S$ Components: t' Spectra

- For each t' bin: integrate intensity of wave components over fitted $m_{3\pi}$ range
- Fit t' spectrum with simple model: $\mathcal{I}_j(t') = A_j \cdot (t')^{|M|} \cdot e^{-b_j\,t'}$
  - Slope parameter b_j

$a_1(1260)$ | $a_1(1640)$ | non-resonant

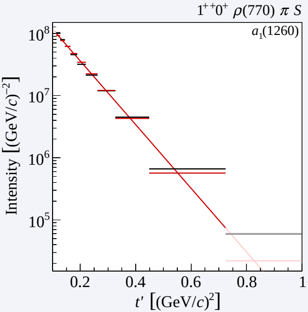

$b = (11.8\,^{+0.9}_{-4.2})\ (\mathrm{GeV}/c)^{-2}$ | $b = (7.7\,^{+6.2}_{-0.4})\ (\mathrm{GeV}/c)^{-2}$ | $b = (12.5\,^{+2.1}_{-1.5})\ (\mathrm{GeV}/c)^{-2}$

$1^{++}0^{+}\rho(770)\,\pi\,S$ Components: t' Spectra

[arXiv:1802.05913]

- For each t' bin: integrate intensity of wave components over fitted $m_{3\pi}$ range
- Fit t' spectrum with simple model: $\mathcal{I}_j(t') = A_j \cdot (t')^{|M|} \cdot e^{-b_j t'}$
  - Slope parameter b_j

$a_1(1260)$

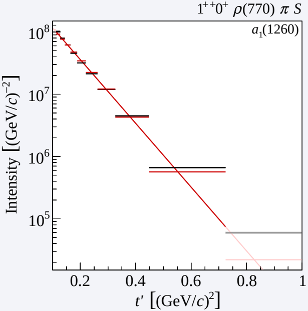

$b = (11.8\,^{+0.9}_{-4.2})\ (\mathrm{GeV}/c)^{-2}$

$a_1(1640)$

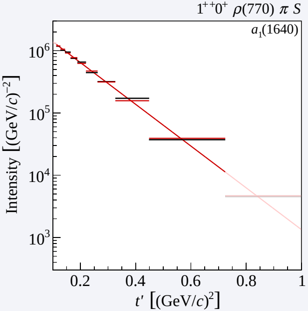

$b = (7.7\,^{+6.2}_{-0.4})\ (\mathrm{GeV}/c)^{-2}$

non-resonant

$b = (12.5\,^{+2.1}_{-1.5})\ (\mathrm{GeV}/c)^{-2}$

$1^{++}0^{+}\,\rho(770)\,\pi\,S$ Components: t' Spectra

[arXiv:1802.05913]

- For each t' bin: integrate intensity of wave components over fitted $m_{3\pi}$ range
- Fit t' spectrum with simple model: $\mathcal{I}_j(t') = A_j \cdot (t')^{|M|} \cdot e^{-b_j t'}$
  - Slope parameter b_j

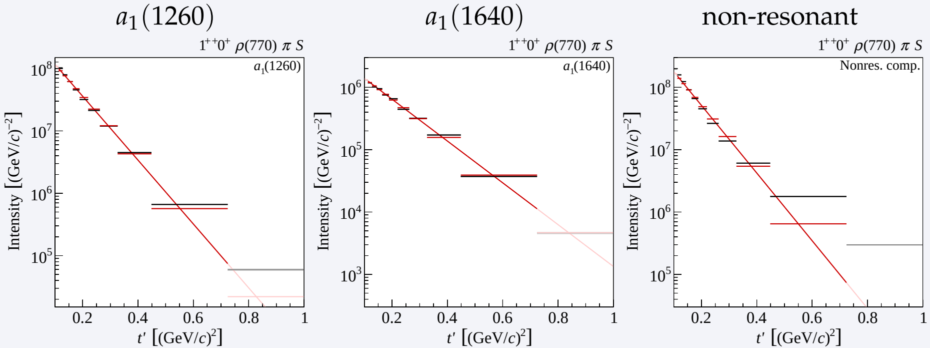

$b = (11.8\,^{+0.9}_{-4.2})\ (\mathrm{GeV}/c)^{-2}$ $\quad b = (7.7\,^{+6.2}_{-0.4})\ (\mathrm{GeV}/c)^{-2}$ $\quad b = (12.5\,^{+2.1}_{-1.5})\ (\mathrm{GeV}/c)^{-2}$

$1^{-+}1^{+}\rho(770)\,\pi\,P$ Components: t' Spectra

- For each t' bin: integrate intensity of wave components over fitted $m_{3\pi}$ range
- Fit t' spectrum with simple model: $\mathcal{I}_j(t') = A_j \cdot (t')^{|M|} \cdot e^{-b_j t'}$

Standard fit

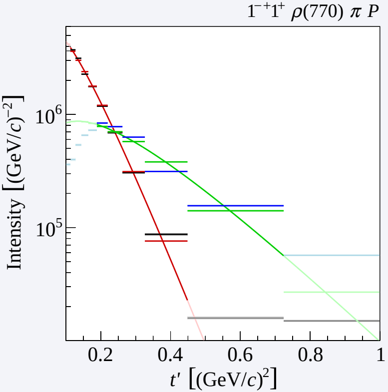

$b_{\text{non.-res.}} = (19.1\,^{+1.4}_{-4.7})\,(\mathrm{GeV}/c)^{-2}$

Deck model used for non-resonant

$b_{\pi_1(1600)} = 7.3\,(\mathrm{GeV}/c)^{-2}$

$1^{-+}1^{+}\rho(770)\,\pi\,P$ Components: t' Spectra

- For each t' bin: integrate intensity of wave components over fitted $m_{3\pi}$ range
- Fit t' spectrum with simple model: $\mathcal{I}_j(t') = A_j \cdot (t')^{|M|} \cdot e^{-b_j t'}$

Standard fit

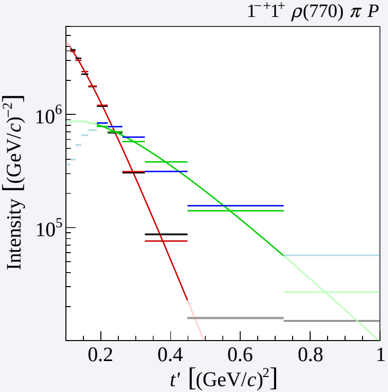

$b_{\text{non.-res.}} = (19.1\,^{+1.4}_{-4.7})\,(\mathrm{GeV}/c)^{-2}$

Deck model used for non-resonant

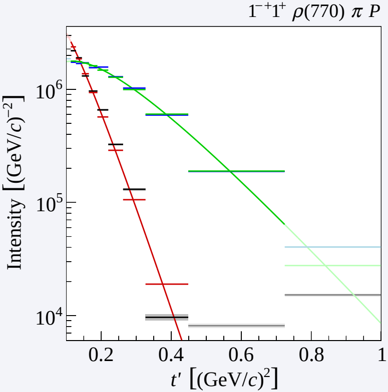

$b_{\pi_1(1600)} = 7.3\,(\mathrm{GeV}/c)^{-2}$

Relative Phases of Wave Components

- Approximately independent of t'
- Consistent with common production mechanism